DESIGN OF FIBER OPTIC SENSOR FABRICATION SYSTEM USING ELECTRIC ARC

LIAU TET LOONG

A project report submitted in partial fulfilment of the requirements for the award of the degree of Bachelor of Engineering (Hons) Electronic Engineering

Faculty of Engineering and Green Technology
Universiti Tunku Abdul Rahman

August 2011

DECLARATION

I hereby declare that this project report is based on my original work except for citations and quotations which have been duly acknowledged. I also declare that it has not been previously and concurrently submitted for any other degree or award at UTAR or other institutions.

Signature : _____

Name : LIAU TET LOONG

ID No. : 08AGB01573

Date :

APPROVAL FOR SUBMISSION

I certify that this project report entitled **"DESIGN OF FIBER OPTIC SENSOR FABRICATION SYSTEM USING ELECTRIC ARC"** was prepared by **LIAU TET LOONG** has met the required standard for submission in partial fulfilment of the requirements for the award of Bachelor of Engineering (Hons) Electronic Engineering at Universiti Tunku Abdul Rahman.

Approved by,

Signature : _____

Supervisor : MR. DANIEL YONG YUN THUNG

Date : _____

ACKNOWLEDGEMENTS

Author would like to thank everyone who had contributed to the successful completion of this project. Author would like to express the deepest gratitude to supervisor, Mr. Daniel Yong Yun Thung for his invaluable advice, guidance and his enormous patience throughout the development of the research.

In addition, author would also like to express my gratitude to my loving parent and friends who had helped and given me encouragement to complete this project

Next, author would like to thank laboratory assistant, Mr. Thong Marn Foo for his support, printed circuit board progressing, and miscellaneous in the lab.

Lastly, author would like to thank lecturer, lab assistants and friends who provided support and help during the project execution.

DESIGN OF FIBER OPTIC SENSOR FABRICATION SYSTEM USING ELECTRIC ARC

ABSTRACT

Fiber optic sensors which become a useful technology connected with the optoelectronic manufacture and fiber optic communications field. The ability of fiber optic sensors to replace the traditional sensors and the sensor applications technology has been improved at this moment such as field and wave measurement, pressure, acoustics, temperature, vibration, humidity and medical measurements. The project focuses on design of long period grating fabrication system. The fabrication principle of the long period fibre grating is based on the electric arc technique. Author is using a simple ways to develop an electric arching driver system by using 12 V from power supply for generating electric arc by using a common car ignition coil. Other than that, author design a whole system of the fabrication with holding fiber optic cable with spark gap and using graphical programming, LabVIEW Software to control the aligner for align the fiber optic cable. Besides that, author was developed connectorization and polishing optical fiber to contribute this project. SLED driver board are used as broadband sources to transmit a wavelength pass through optical fiber and spectrometer are accept the light then graphic display at specific operating software. The results demonstrate that provide grating data in the project. The progress of design, methodology, implementation, testing and measurement are discussed here.

TABLE OF CONTENTS

DECLARATION ii
APPROVAL FOR SUBMISSION iii
ACKNOWLEDGEMENTS v
ABSTRACT vi
TABLE OF CONTENTS ii
LIST OF TABLES x
LIST OF FIGURES xi
LIST OF SYMBOLS / ABBREVIATIONS xiv
LIST OF APPENDICES xv

CHAPTER **PAGE**

1 INTRODUCTION **1**
1.1 Background 1
1.2 Aims and Objectives 2
1.3 Report's Guidance 2

2 LITERATURE REVIEW **4**
2.1 Long Period Fiber Grating Sensors (LPFGs) 4
2.1.1 LPFGs Theory 6
2.1.2 LPFG fabrication 6
2.2 Summary 8

3 RESEARCH METHODOLOGY **9**
3.1 Methodology 9
3.2 Project Design 9

CHAPTER **PAGE**

3.2.1 Electric Arcing Driver System 10
3.2.1.1 Electric Arcing Schematic Diagram 11
3.2.1.2 EMI Protecting for Ignition Coil Circuit 12
3.2.1.3 Completed Schematic Diagram 14
3.2.2 Development Electric Arcing System Driver to PCB 14
3.2.2.1 PCB Fabrication Process Details 14
3.2.3 Ignition Coil 19
3.2.4 Spark Gap 20
3.2.4.1 Distance between Both Spark Gap 21
3.2.5 Motorized Translation Stages (Aligner) 22
3.2.5.1 A Module Holds Spark Gap with Aligner 23
3.2.6 LabVIEW 24
3.2.6.1 APTUser Utility 25
3.5.6.2 APT within LabVIEW 26
3.2.6.3 Controller for Aligner 28
3.2.7 SFG-830 29
3.2.7.1 SFG-830 within ARB 29
3.2.7.2 SFG-830 within LabVIEW 30
3.2.8 Connectorization and Polishing Optical Fiber 31
3.2.8.1 Fiber Optic Cable Assembly Process Details 31
3.2.8.2 Fiber Polishing Assembly Process Details 35
3.2.9 SLED Driver Board EDB5080 38
3.2.9.1 Operating EDB5080 38
3.2.10 Spectrometer SM242 40
3.2.10.1 SM32ProForUSB 41
3.3 Overview of the Project 42

4 RESULTS AND DISCUSSIONS 43
4.1 Testing and Measurement 43
4.1.1 Testing and Measurement Electric Arcing Driver Circuit 43

CHAPTER **PAGE**

4.1.1.1 Output Waveform 44
4.1.1.2 Output Voltage 45
4.1.2 Testing Ignition Coil and Measuring Spark 45
4.1.3 Testing and Measurement Electric Arcing Driver Circuit after Developed in PCB 47
4.1.4 Testing and Measuring Spark after Developed in PCB 48
4.2 Running a Virtual Instrument (VI) with APT by LabVIEW 49
4.2.1 Testing Electric Arcing Driver and Running VI with APT Parallel 50
4.3 Running SFG-830 within LabVIEW 50
4.4 Testing Optical Fiber with Connector 51
4.4.1 Measuring Optical Fiber Cable by Using Optical Power Meter 52
4.4.2 Measuring Optical Fiber Cable by Using SM32ProForUSB 53
4.5 Testing Optical Fiber after Grating 55
4.5.1 Grating Data 55

5 CONCLUSION AND RECOMMENDATIONS 58
5.1 Conclusion 58
5.2 Recommendations and Future Development 59

REFERENCES 61

APPENDICES 63

LIST OF TABLES

TABLE	TITLE	PAGE
3.16	The Characteristics of Two Different Distances	22
4.18	Grating Data for Two Types of Setting	56

LIST OF FIGURES

FIGURE	TITLE	PAGE
2.1	Schematic of LPFG	4
2.2	Modulated Reference Fiber Grating	5
2.3	LPFG Forward Cladding Modes	5
2.4	LPG Fabrication using UV Laser	7
2.5	Corrugated Fiber LPFG	8
3.1	Overall Author's Experience Set Up	10
3.2	Electric Arcing Driver System	11
3.3	Electric Arcing Schematic Diagram	12
3.4	EMI Protection for Electric Arcing Driver	13
3.5	Complete Electric Arcing Schematic Diagram	14
3.6	PCB Process Flow Chart	15
3.7	Schematic Diagram of Electrical Arching System Driver	16
3.8	Layout of Electric Arching System Driver	16
3.9	Board Layers Printed	17
3.10	Overview the PCB Board	18
3.11	Electric Arcing System Driver	18
3.12	Ignition Coil	19
3.13	Ignition Coil as Transformer	20

FIGURE	TITLE	PAGE
3.14	Spark Gap Electrodes	21
3.15	Distance between Spark Gap Electrodes	21
3.17	Motorized Translation Stages (Aligner)	23
3.18	Module holds Spark Gap with Aligner	24
3.19	Aligner with Module	24
3.20	APTUser Utility	25
3.21	Interface front panel with Motor Controller	27
3.22	Block Diagram of Motor Controller	28
3.23	Manual Controller	28
3.24	SFG-830 Using ARB Editing Software	29
3.25	Front Panel Window of SFG-830 Function Generator	30
3.26	Block Diagram of SFG-830 Function Generator	30
3.27	Fiber Optic Cable Assembly Process Flow Chart	31
3.28	Optical Fiber	32
3.29	FC Connector	32
3.30	Epoxy	34
3.31	Epoxy Bead	34
3.32	Fiber Polishing Assembly Process Flow Chart	35
3.33	Scoring the Optical Fiber	36
3.34	Polishing Steps	37
3.35	Overview Optical Fiber with FC Connector	37
3.36	SLED Driver Board EDB5080	38
3.37	SLED Current Adjusted through Potentiometer	39

FIGURE	TITLE	PAGE
3.38	Spectrometer SM242	40
3.39	SM32Pro Operating Software	41
3.40	Overview of the Whole Project	42
4.1	Measurement of Electric Arcing Driver Circuit	44
4.2	Output Waveform	44
4.3	Output Voltage	45
4.4	Testing Ignition Coil Schematic Diagram	46
4.5	Ignition Coil System	46
4.6	Spark Generated by Ignition Coil	47
4.7	Measurement Electric Arcing Driver Circuit after Develop in PCB	48
4.8	Electric Spark	48
4.9	VI with Live Data	49
4.10	Error Problem Synchronize LabVIEW with SFG-830	50
4.11	Multifunction Loss Tester	51
4.12	Magnified Views of Optical Fiber Connector	52
4.13	Output Power of SLED Driver Board	52
4.14	Output Power after Pass through Optical Fiber Cable	53
4.15	Output Wavelength of SLED Driver Board	54
4.16	Output Wavelength after Pass through Optical Fiber Cable	54
4.17	Grating Process Using Electric Spark	55
4.19	Grating Data Before and After Grating	56

LIST OF SYMBOLS / ABBREVIATIONS

λ_{res}	resonance of the LPFG
$n_{co,eff}^{01}$	the effective indices of the fundamental core mode
$n_{cl,eff}^{m}$	the *m* th cladding mo
Λ	the period of grating
L	the length of the LPG
κ_i	the coupling coefficient for the *i* th cladding mode
V_{pp}	voltage peak-to-peak
LPFG	long period fiber grating
UV	ultraviolet
DDS	direct digital synthesis
EMI	electromagnetic interference
DC	direct current
PCB	printed circuit board
EMF	electromagnetic field
OS	operating system
PLC	programmable logic controller
NI	National Instrument
OPC	OLE for process control
CPU	central processing unit
VISA	virtual instrument software architecture
VI	virtual instrument
FC	fixed connection
TEC	temperature controller
SLED	luminescent light emitting diode
CCD	charge coupled device
GPIB	general purpose interface bus

LIST OF APPENDICES

APPENDIX	TITLE	PAGE
A	Final Year Project Gantt Chart	63
B	Final Year Project Process Flow Chart	63
C	BFY 50/51 Datasheet	64
D	2N3055 Datasheet	70
E	Motorized Translation Stages Installation	75
F	SM242 Specification	81
G	EBD 5000 Driver Board Specification	84

CHAPTER 1

INTRODUCTION

1.1 Background

Fiber optic sensor, which become a useful technology connected with the optoelectronic manufacture and fiber optic communications field. A lot of fiber optic sensor applications have been developed with many components to support major industries [1-2].

Most ability of fiber optic sensors to force replaces the traditional sensors and the sensor applications technology has been improve at this moment such as field and wave measurement, pressure, acoustics, temperature, vibration, humidity and medical measurements [3].

Nowadays, fiber optic sensor technology is directly extremely archived at markets. The advantages of fiber optic sensors contain of small size, low power consumption and not damaging effect with electromagnetic signal interference so it ability suitable to be lightweight. Besides that, the fiber optic sensors have a high sensitivity, bandwidth and environmental future show that it's strongly offshoot capable of propagation of ultimate user not acquainted and costly high [4].

Ultraviolet writing in fiber gratings is the course concentration influence that moves it come the need for new technology, high performance fiber grating devices to increase the bandwidth for high speed telecommunication in network systems, the utilization of fiber grating technology as an optical sensing has boost

speed of transfer [5]. Moving forward, fiber grating devices in telecommunications fields will ensure a continuing reduction in the cost of the technology that will encourage the expanding of sensing applications using fiber optic grating sensor devices or systems.

Furthermore, the evolution of integrated fiber optic sensors made a lot benefit to development some smart part of organism, leading a head to improvements in safety and economic such as civil works, road and rail bridges, tunnels, dams, maritime structures, airframe sections, projectile delivery systems, and numerous medical appliances [6].

1.2 Aims and Objectives

The project aims to study the design methodology of fiber optic sensor for detect the temperature, strain and PH. The main objective of this project is to study the design of long period grating fabrication system. This project requires kind of knowledge's such as function generator, oscilloscope, circuit theory, transistor specification and ignition coil for first part of author project. This is following by developing of the electric arcing system for grating fiber optic.

Other objective is using graphical programming, LabVIEW Software to control the aligner for align the fiber optic cable and function generator create a signal to an electric arcing circuit for generating a spark while the system in progress. Both part will running parallel.

1.3 Report's Guidance

Chapter 1 is the introduction that gives an overview of fiber optic sensors that includes the basic concepts, development, and some of the classic applications. The background, aims and objectives, and report's guidance has been state here.

Chapter 2 is the literature review that includes some reference sources such as theories, articles and reference books information. Here is summarizing some author material, ideas, information, data, principle knowledge, components characteristic and properties.

Chapter 3 is describing about research methodology to. The design method and algorithms to implement and develop in this project. Further root analysis and solution planning is couple with the methodology used in this project. The hardware progress for electrical arching driver and setup the project are present.

Chapter 5 is showing the results and discussion. The measurement data and discussion is representing in the chapter to prove the result.

Chapter 6 is conclusion and recommendation. This chapter summarizes the entire project, discussed the problem and solutions with planning task for future work.

Bibliography is a list of references of the resources that author used Appendix like components datasheet, instrument specifications and so on.

CHAPTER 2

LITERATURE REVIEW

2.1 Long Period Fiber Grating Sensors (LPFGs)

LPFGs have modulated refractive index periods typically in a range of 50 m until 500 m. The LPFG has a period typically in the range 100 μm to 1 mm, as illustrated in Figure 2.1. LPFGs are capable of coupling light between the forward propagating cores and cladding modes, generating a series of attenuation resonance peaks in transmission [7]. Therefore, the ability an essential low level of back reflection and it's inexpensive to produce. LPFG based devices and systems have been demonstrated for a multitude of applications in optical fiber communications and sensing.

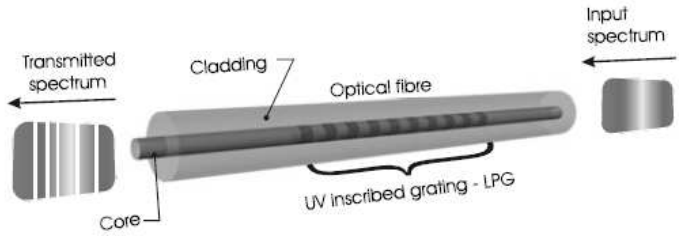

Figure 2.1: Schematic of LPFG

The actual of light coupling contain of cladding modes emphasize that the LPFG spectral response is powerful to sway by the optical properties of the cladding and the surrounding fiber optic medium. It's also sensitivity to the external refractive index is advantage for chemical sensing applications [8]. Other sensing devices with sensitivity advantages include optical load and bend sensors [9]. These sensors are more specifically as the sensing mechanism is based on a

perturbation encoded resonance mode splitting measurement rather than conventional wavelength shifting detection [10].

Fiber grating demodulation systems require very high resolution spectral measurements shown in Figure 2.2. One way to accomplish this is to beat the spectrum of light reflected by the fiber grating against the light transmission characteristics of a reference grating.

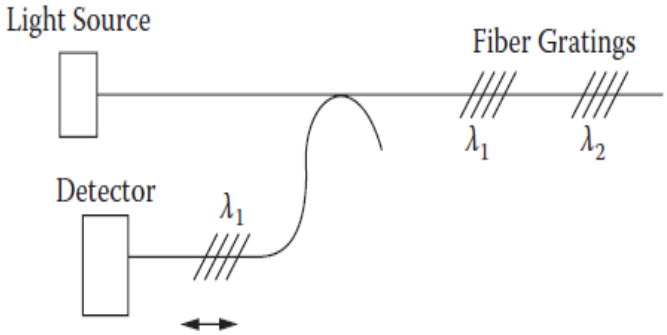

Figure 2.2: Modulated Reference Fiber Grating

A LPFG can couple the forward propagating core mode to one or a few of the forward propagating cladding modes in Figure 2.3.

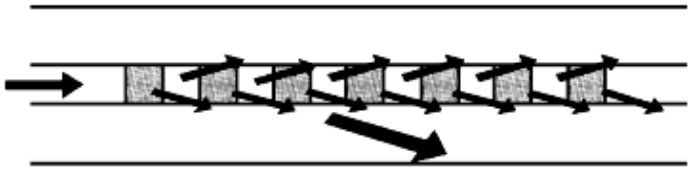

Figure 2.3: LPFG Forward Cladding Modes

The sensitivity to a particular measuring is dependent upon the composition of the fiber and upon the order of the cladding mode, to which the guided optical power is coupled, and is thus different for each attenuation band. This range of responses makes them particularly attractive for sensor applications, with the prospect for multi parameter sensing using a single sensor element [11].

2.1.1 LPFGs Theory

The long periodicity of LPFG results in light coupling from the core mode to the discrete cladding modes. The coupled cladding modes attenuate rapidly as they propagate along the length of the fiber due to the lossy cladding surrounding interface and bends in the fiber. Consequently, a series of attenuation resonance bands is generated only in transmission. The resonance of the LPFG, λ_{res}, occurs only at the phase match condition

$$\lambda_{res} \left(n_{co,eff}^{01} - n_{cl,eff}^{m}\right)\Lambda$$

where $n_{co,eff}^{01}$ and $n_{cl,eff}^{m}$ are the effective indices of the fundamental core mode and the *m* th cladding mode, respectively, and Λ is the period of grating [12].

The minimum transmission of the attenuation bands is governed by the expression

$$T_i = 1 - sin^2(\kappa_i L)$$

where L is the length of the LPG and κ_i is the coupling coefficient for the i th cladding mode, which is determined by the overlap integral of the core and cladding mode and by the amplitude of the periodic modulation of the mode propagation constants [13].

Any modulation of the core and cladding guiding properties will modify the spectral response of LPFGs, which is essential for sensing purposes. The external perturbations are detected as wavelength dependent loss modulation of an LPFG.

2.1.2 LPFG fabrication

The fabrication of LPFGs relies upon the introduction of a periodic modulation of the optical properties of the fiber. This may be achieved by permanent modification of the refractive index of the core of the optical fiber or by physical deformation of the fiber [14]. The modulation of the core refractive index has been achieved by ultraviolet (UV) irradiation [15]. The UV induced

index modulation is typically achieved in Ge doped silica fibers using wavelengths between 193 *n*m and 266 *n*m [16]. This is the most widely utilized method for the fabrication of LPFGs. The refractive index change is associated with the formation of Ge related glass defects. A typical LPG fabrication configuration, using UV irradiation through an amplitude mask is shown in Figure 2.4.

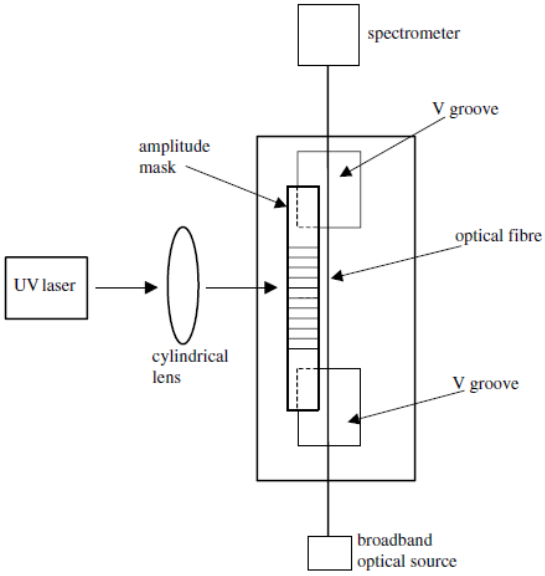

Figure 2.4: LPG Fabrication using UV Laser

The output from a UV laser source is used to illuminate the optical fiber through an amplitude mask of appropriate period, which may be fabricated in chrome plated silica [17] or from a metal foil. The cylindrical lens produces a line focus oriented parallel to the axis of the fiber.

Electric arc fabrication of an LPFG relies upon a combination of up to four effects to generate the periodic modulation of the fiber properties. The mechanisms exploited include the induction of micro bends into the fiber [18], the periodic tapering of the fiber [19]. Typically, the electrodes of a fusion splicing machine are used, exposing a region of fiber with a length of the order of 100 μm to the arc, limiting the minimum period of LPFG that may be fabricated. The corrugated fiber is shown in Figure 2.5. When a tensile load is applied to the fiber, the periodic variation in the diameter of the fiber results in a periodic strain

variation across the corrugated structure, with a concomitant periodic refractive index induced via the photo elastic effect. Thus the coupling strength increases with applied load, with a small change in wavelength of the attenuation bands [20].

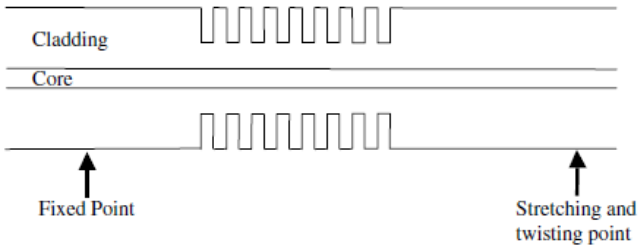

Figure 2.5: Corrugated Fiber LPFG

Generally, LPGs have been fabricated to operate at telecommunications wavelengths that are 1300 *n*m and 1550 *n*m. The spectrum is monitored by coupling light from super fluorescent fiber sources or super luminescent diodes in the fiber and recording the transmission using an optical spectrum analyzer. There have been reports of the use of fibers with lower cutoff wavelengths, 650 *n*m, allowing the operation of the LPFG within the response of silicon detectors, facilitating the use of low cost CCD spectrometers [21].

2.2 Summary

The sensitivity of LPFGs to strain, temperature, PH the ability to tune the sensitivity by virtue of fiber composition and LPFG period, and the presence of features with the transmission spectrum that show differing sensitivities to the various measured offer the prospect for the development of sensor elements capable of simultaneously and independently monitoring a number of measured. That means for optimizing the performance of the LPFG for particular applications has been outlined, along with a review and research of the uses to which they have been put [22].

CHAPTER 3

RESEARCH METHODOLOGY

3.1 Methodology

There is a lot of methodology can be choose doing this project such as which kind of function generator, power supply, components availability for the circuits, frequency stability for the system, and the suitability of methodology of the author. Author will make a decision base on doing a lot of research by doing testing and measurement describe in next chapter.

3.2 Project Design

Overall the design for this project is fiber optic sensor detect the temperature, strain and PH. This project included a lot of appliances such as function generator, oscilloscope, electric arching driver circuit, ignition coil for first part of author project to develop an electric arcing system for grating the fiber optic.

Overall the design for second part of this project is design a whole system of the fabrication with holding fiber optic cable and using graphical programming, LabVIEW Software to control the aligner for align the fiber optic cable and control the function generator to create a signal to an electric arcing driver circuit for generating spark to grating a fiber optic cable while the system in progress. The overall author's experiment set up will be shown in Figure 3.1.

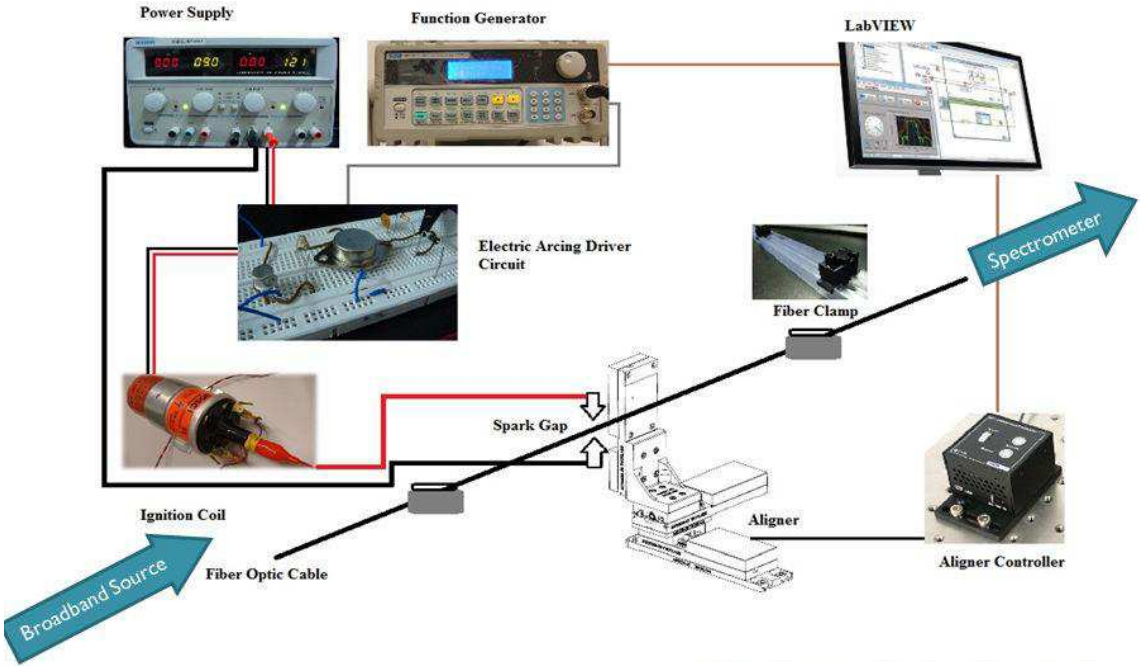

Figure 3.1: Overall Author's Experience Set Up

3.2.1 Electric Arcing Driver System

An ignition system is a system for igniting a fuel air mixture. It is best known in the field of internal combustion engines but also has other applications, such as oil fired and gas fired boilers [23]. The earliest internal combustion engines used a flame, or a heated tube, for ignition but this is quickly replaced by systems using an electric spark.

Author is using a simple ways to develop an electric arching driver system by using 12 V from power supply for generating electric arc by using a common car ignition coil. An electric arc is an electrical breakdown of a gas which produces an ongoing plasma discharge, resulting from a current flowing through normally nonconductive media such as air. A synonym is arc discharge that characterized by a lower voltage than a glow discharge, and relies on thermionic emission of electrons from the electrodes supporting the arc [24].

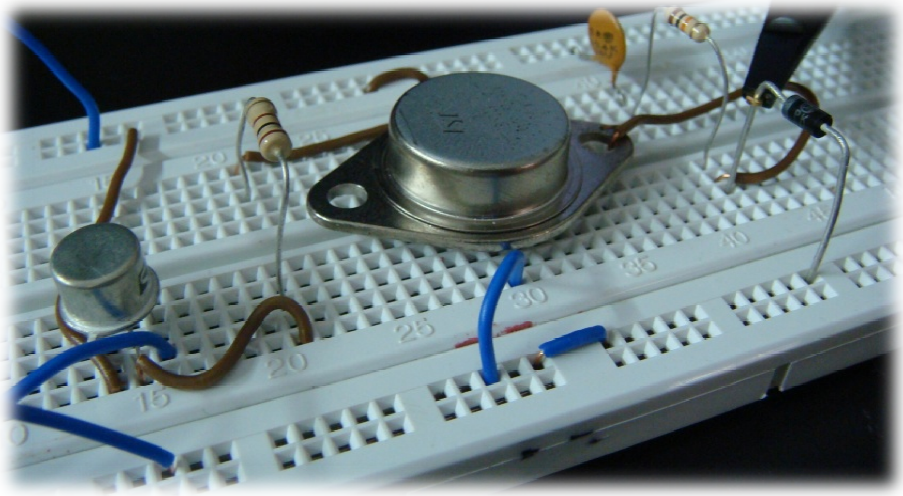

Figure 3.2: Electric Arcing Driver System

3.2.1.1 Electric Arcing Schematic Diagram

Base on some references and component specifications, some research and guidance has made the author chosen the DDS function generator to replace the 555 Timer IC. So it will be more reliability by using software and easy to control than using on off button. The frequency range to generate a clock signal for the circuit will be 100 Hz to 500 Hz, which depend on how long need to generate the spark. The amplitude of the function generator will be set at least 4 V_{pp} and maximum 10 V_{pp} so the power supply has enough current to power up the ignition coil.

Some components has been chosen for the circuit such as the commonly used 2N3055 transistor due to it high power switching capability because the 2N3055 is cheap and high temperature tolerant, so this component are susceptible to voltage spikes caused by the inductive nature of the ignition coil load. Ones with higher voltage ratings will be less likely to be damaged by spikes. The electric arching schematic diagram shown at Figure 3.3 has listed out all the components.

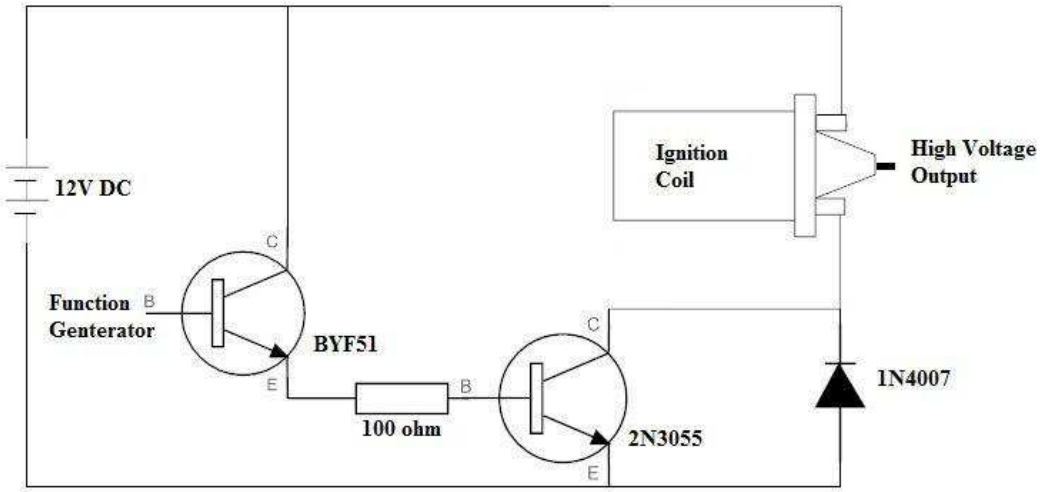

Figure 3.3: Electric Arcing Schematic Diagram

Figure 3.3 diagram shows how a BFY51 transistor is use as a switch for controlling the high frequency signal is allow getting to the power transistor. While 0 V placed on the modulation input, the high frequency signal will be blocked and the power transistor will switch off.

When some voltage is apply to the modulation input, the high frequency signal can pass through and drive the power transistor. The level of the high frequency signal reaching the power transistor will be proportional to voltage applied to the modulation input. Therefore if the modulation input voltage is varying with time, the output power of the ignition coil at the electric arcing driver frequency will vary with it.

3.2.1.2 EMI Protecting for Ignition Coil Circuit

The build of electric arc circuit to power up ignition coil to make a high voltage sparks and arcs, the circuit should need some sort of electromagnetic interference (EMI) protection. Without EMI protection, the ignition coil likely will destroy the transistors or other components.

In general should to reduce an electromagnetic interference or voltage spikes. A lot of ways to reduce EMI and it can often be useful to use various stop

in different parts of the circuit. This electric arc circuit diagram represents a few possible ways you can snub EMI in an electric arc circuit. This is known as dissipative stop because the excess energy is dissipated as heat or light.

Try to create a series connected capacitor and resistor shown in Figure 3.4. The resistor will prevent the transistor from blowing and the capacitor will block DC. The values used will depend on your drive frequency. Normally, a bigger capacitance and smaller resistance will snub more, but also absorb more electric arc circuit power cause the system reducing efficiency. A compromise value of component must be found that best suits for the setup. The RC circuit does work to absorb spikes but it is going to reduce the possible output voltage of the coil. When the capacitor is charged or there is nothing on the output of the coil there will be more EMF because the energy is reflected back.

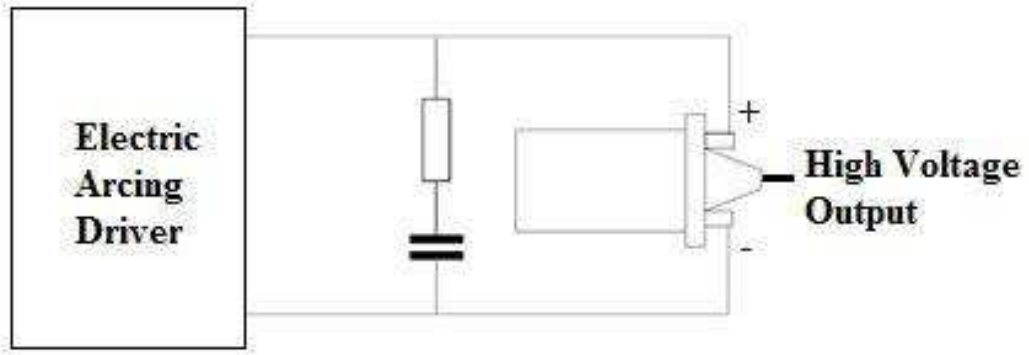

Figure 3.4: EMI Protection for Electric Arcing Driver

3.2.1.3 Completed Schematic Diagram

The following electric arching circuit diagram shown in Figure 3.5 was finalized and completed under protects.

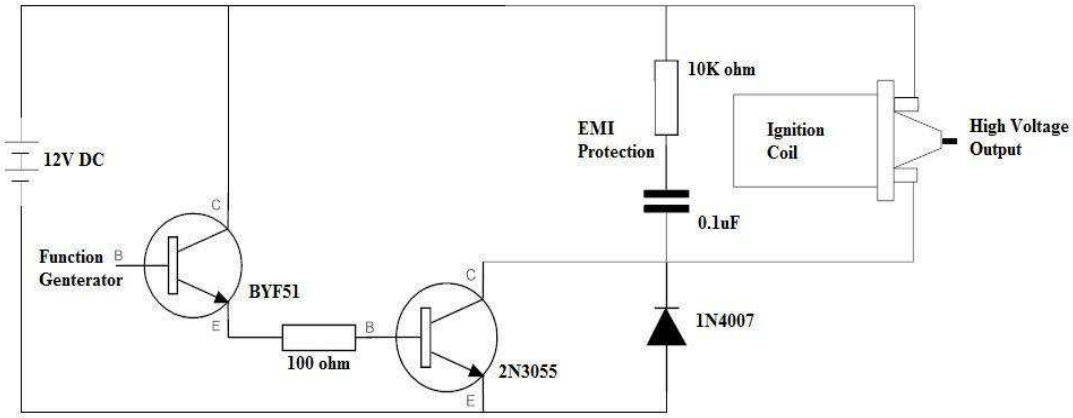

Figure 3.5: Complete Electric Arcing Schematic Diagram

3.2.2 Development Electric Arcing System Driver to PCB

Author was developed an electric arcing driver system fabricated on PCB because breadboard was noisier and not a good conductor. It also does not support frequencies as high as properly and take up more physical space than the PCB.

3.2.2.1 PCB Fabrication Process Details

While making PCB isn't particularly difficult and isn't a trivial undertaking. Author need to acquire some kind of PCB layout program, and some specialized equipment. There is also a bit of a learning curve to it, especially the PCB layout tool. The PCB process flow chart was shown in Figure 3.6.

Figure 3.6: PCB Process Flow Chart

Author was using EAGLE PCB software by CadSoft. The first step was transfer the schematic from the circuit to the schematic part of the layout program shown in Figure 3.7.

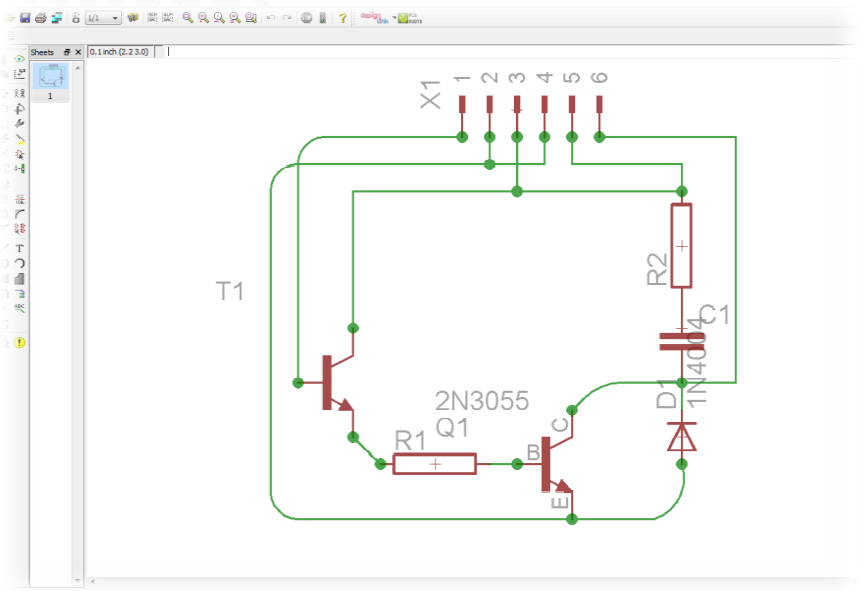

Figure 3.7: Schematic Diagram of Electrical Arching System Driver

After the schematic was entered, the PCB layout program was used to place the parts on the board and route the copper traces. After the first few parts were routed, the "rats nest" begins to clear up shown in Figure 3.8.

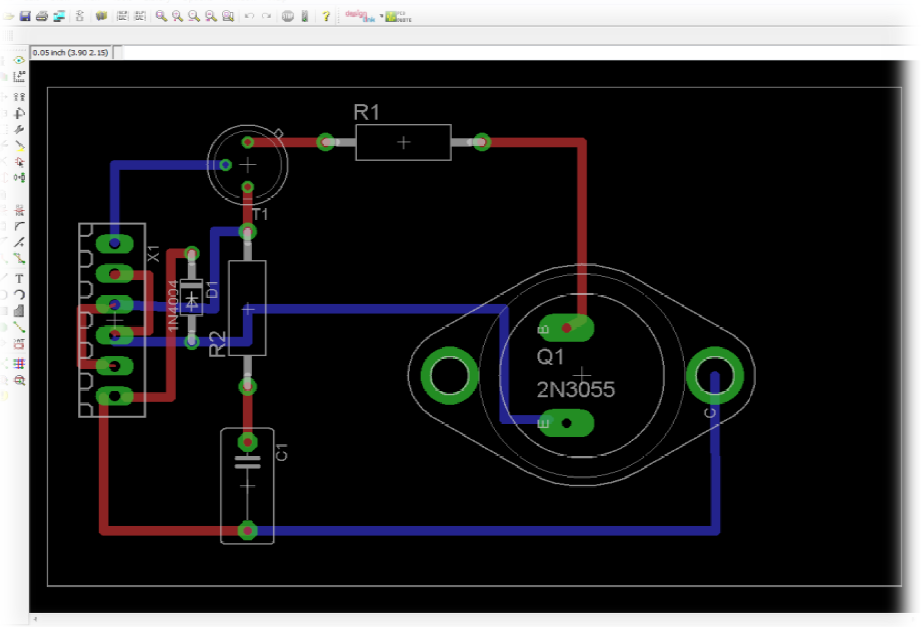

Figure 3.8: Layout of Electric Arching System Driver

When the layout was done, the board layers were printed onto special toner transfer paper with a laser printer shown in Figure 3.9.

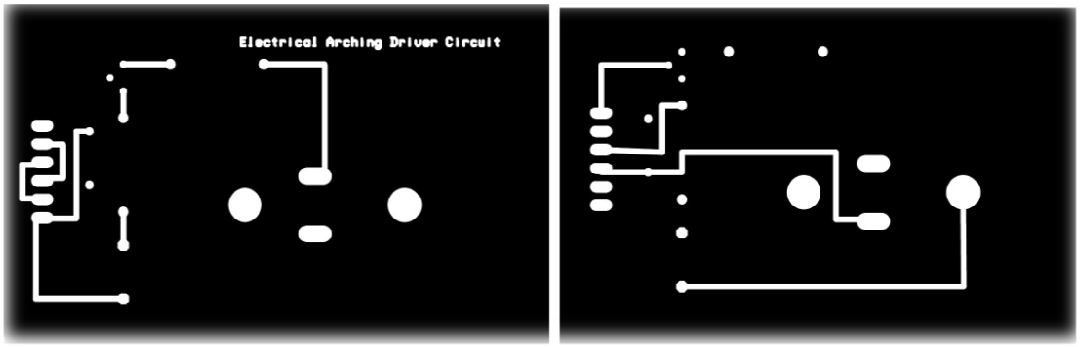

Figure 3.9: Board Layers Printed

After that, author prepared a double sided PCB for fabrication. CNC machine which was a high speed drilling machine used to drill required mounting hole onto PCB. It's required precision placement and was done by automated drilling machine, driven by drill files. The next step was plated the holes with conducting copper for conductive between top and bottom layer.

A UV light ray was projected onto a substrate through the master pattern mask to create the circuit pattern. This board "image" was transferred to the bare copper board with a laminating machine. The blue tenting dry film surface was coated with a photosensitive chemical known as resist. After laminating, developing fluid was used to melt the unexposed resist, leaving the exposed circuit pattern intact. The board with the paper stuck to it was soaked to remove the paper, leaving only the toner behind.

After the transfer paper has been soaked off. Inside the etch tank, two aquarium pumps circulate etchant over the copper boards while two aquarium heaters keep the solution. Etching was used to corrode the portions of the copper foil without resist, carving out the areas around the circuits. After etching part, the toner was removed with solvent and the board was tinned using a soldering iron and a small piece of tinned solder wick. Tinning wasn't absolutely necessary but it improves the appearance of the board, and prevents the copper from oxidizing

before it's solder the parts to the board. The resist which has completed its role as mask was removed as shown in Figure 3.10 below.

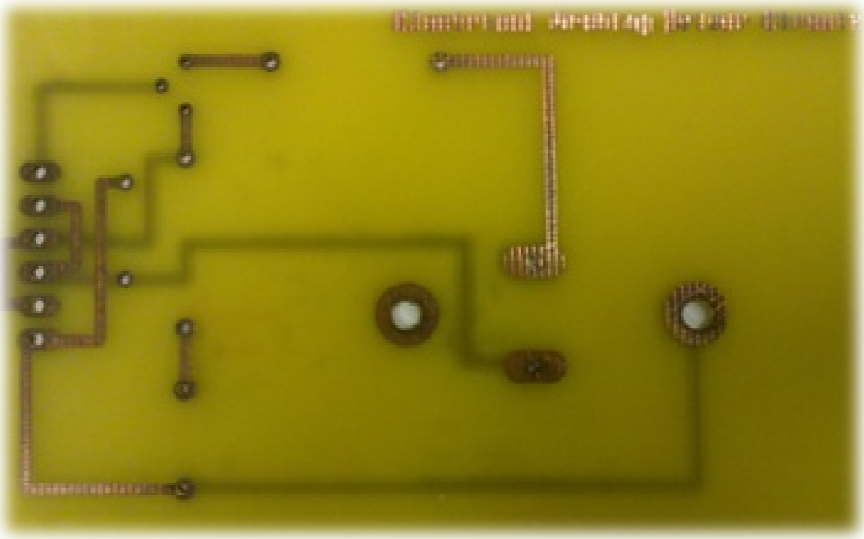

Figure 3.10: Overview the PCB Board

An electric arcing driver system for grating fiber optic was complete fabricated on PCB shown in Figure 3.11.

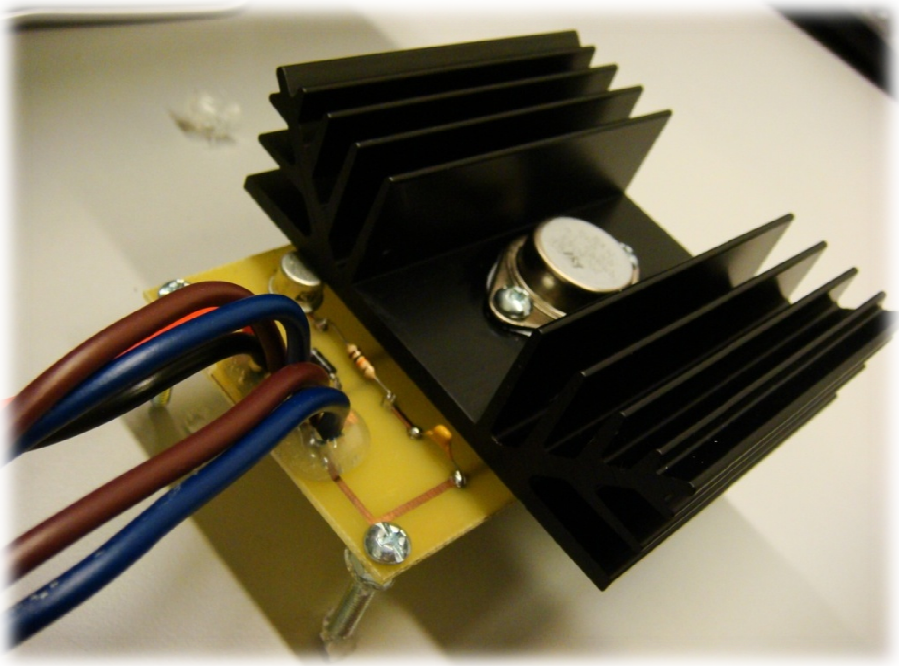

Figure 3.11: Electric Arcing System Driver

3.2.3 Ignition Coil

Ignition coils shown in Figure 3.12 are type of induction transformer based on the Tesla Coil invented by Nikola Tesla in 1891. An ignition coil also called as spark coil which is an induction coil in an automobile's ignition system which transforms the battery's 12 V to the thousands of volts (x 10k) needed to spark the spark plugs. It is used to produce high voltage, low current, high frequency alternating current electricity, although Tesla coils produce higher current than the other source of high voltage discharges, electrostatic machines. Tesla experimented with a number of different configurations and they consist of two, or sometimes three, coupled resonant electric circuits [25].

Figure 3.12: Ignition Coil

The ignition system is designed so that a 12 V battery can generate the very high voltage required to create such a discharge. The heart of this system is a device called an ignition coil. This coil is a kind of transformer. Transformers transfer voltage from one circuit to another, either as a higher voltage or a lower voltage. The key principle that makes transformers work is electromagnetic induction: A moving magnetic field, or a change in a stationary magnetic field, can induce a current in a wire exposed to that field.

This ignition coil is a pulse type transformer. Like other transformers, it consists, in part, of two coils of wire, as shown in the Figure 3.13. These are both wrapped around the same iron core. Because this is a step up transformer, the

secondary coil has far more turns of wire than the primary coil, which is wrapped around the secondary. In fact, the secondary coil has several thousand turns of thin wire, whereas the primary coil has just a few hundred.

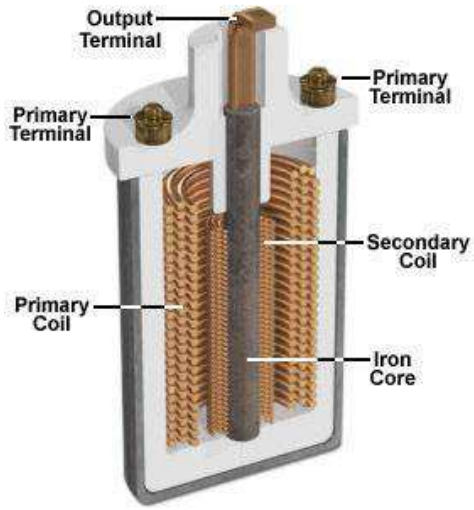

Figure 3.13: Ignition Coil as Transformer

3.2.4 Spark Gap

A spark gap consists of an arrangement of two conducting electrodes separated by a gap usually filled with a gas such as air, designed to allow an electric spark to pass between the conductors. When the voltage difference between the conductors exceeds the gap's breakdown voltage, a spark forms will ionizing the gas and drastically reducing its electrical resistance. An electric current then flows until the path of ionized gas is broken or the current reduces below a minimum value called the 'holding current' [26].

Electric arcs are used for welding, plasma cutting, for electrical discharge machining, as an arc lamp in movie projectors and follow spots in stage lighting. Electric arc furnaces are used to produce steel and other substances. For this project author used electric arc to do grating for fiber optic cable.

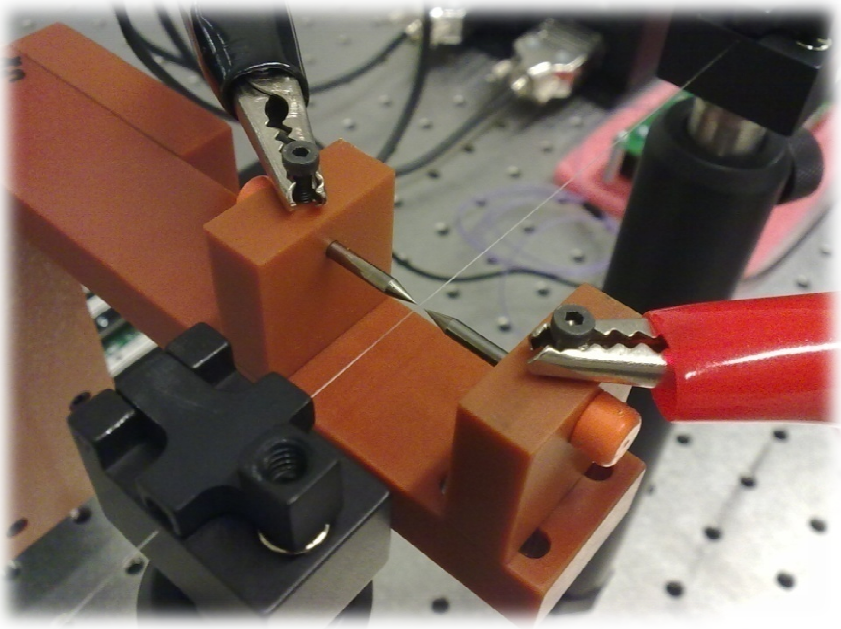

Figure 3.14: Spark Gap Electrodes

3.2.4.1 Distance between Spark Gap

The distance between spark gaps electrodes was determined to contribute of author's project shown in Figure 3.15 below.

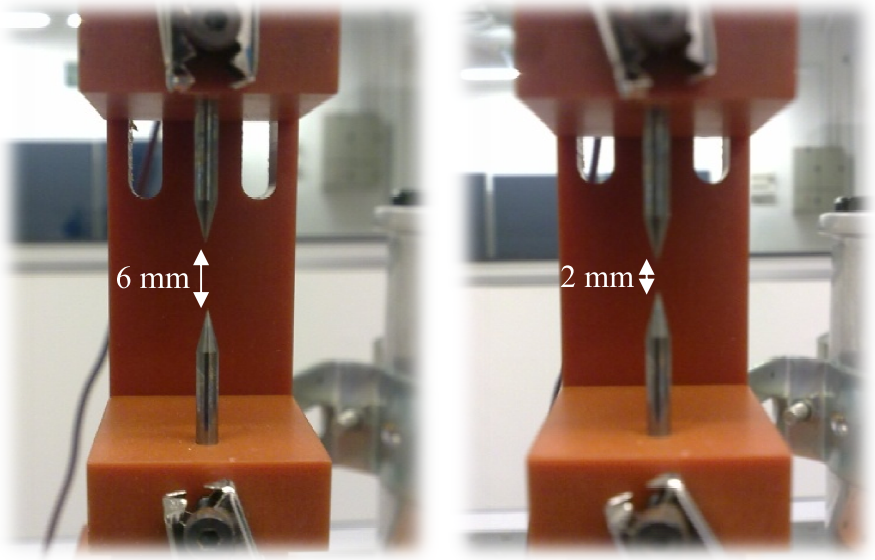

Figure 3.15: Distance between Spark Gap Electrodes

2 mm length was chosen for spark gap because an electric spark looks straight and more focus compare with 6 mm length. The Table 3.16 has shown the characteristics of two different distances current to generate an electric spark with a constant amplitude, V_{pp} = 10.

Short distance (2 mm)			**Long distance (6 mm)**		
V_{pp} = 10	**Current (A)**	**Output electrical spark**	**V_{pp} = 10**	**Current (A)**	**Output electrical spark**
	0.7	Weak		1.6	Weak
	1.0	Standard		2.0	Standard
	1.2	Maintain		2.5	Maintain

Table 3.16: The Characteristics of Two Different Distances

According to Table 3.16, author was using 2 mm distance spark gap in the project. That was because 2 mm only using 1 A to generate standard electric spark however 6 mm need at least 1.6 A to generate weak spark only. While the current set to 2 A, author notices that the minimum amplitude was 4 V_{pp}.

3.2.5 Motorized Translation Stages (Aligner)

The compact motorized MTS Series stages called as aligner shown in Figure 3.17 has feature a dual set of linear rails with continuously recirculation ball bearings on a moveable carriage.

This mechanism provides smooth, low friction movement and ensures high load capacity. The drive power is provided by a DC servo motor. A built in optical encoder provides 12,288 counts per revolution resulting in a minimum incremental motion of less than 50 *n*m.

Figure 3.17: Motorized Translation Stages **(**Aligner)

3.2.5.1 A Module Holds Spark Gap with Aligner

The addition of limit switches on the stage itself ensures controlled motion within the parameters of the unit and prevents overdriving in both directions.

The stages are configurable in XY both left and right handed configurations using spacer plates and angle brackets and XYZ and stage Z as a module to hold a spark gap with aligner.

Base plates allow the stages to be bolted directly to an optical table. For added flexibility, both sizes of travel stages can be configured together either by using LabVIEW software or controller manually.

A module shown in Figure 3.18 was created to hold a spark gap with aligner.

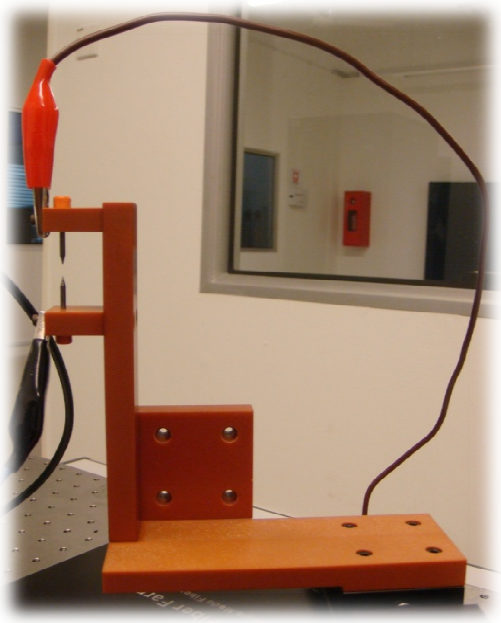

Figure 3.18: Module holds Spark Gap with Aligner

The overall part of aligner combines with a module for author's project shown in Figure 3.19.

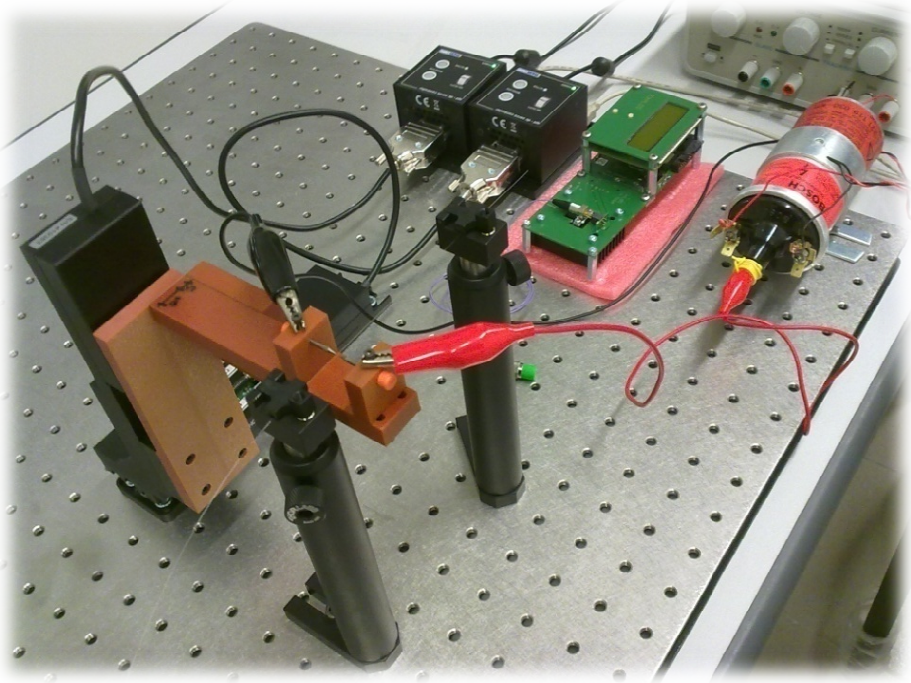

Figure 3.19: Aligner with Module

3.2.6 LabVIEW

LabVIEW is a graphical programming environment used by millions of engineers and scientists to develop sophisticated measurement, test, and control systems using intuitive graphical icons and wires that resemble a flowchart. It offers unrivaled integration with thousands of hardware devices and provides hundreds of built in libraries for advanced analysis and data visualization – all for creating virtual instrumentation. The LabVIEW platform is scalable across multiple targets and OSs, and, since its introduction in 1986, it has become an industry leader.

Author's project wills using this LabVIEW software to control the function generator and control the aligner while fiber grating by electric arcing progressing. LabVIEW software will add advanced analysis and control functionality available to programmable automation controllers to any PLC using the new NI OPC servers. Additionally, the software will find out about debugging connectivity issues using OPC diagnostics.

3.2.6.1 APTUser Utility

APTUser utility is the software to control the aligner. The APT server reads in the stage and controller information on boot up and the settings made above are displayed in the 'Setting' window.

Figure 3.20: APTUser Utility

3.2.6.2 APT within LabVIEW

Programmers of LabVIEW through the use of ActiveX technology, used within the APT platform, can communicate and control any APT controller. By simply specifying which controller to be used within code function calls, properties and events can be used to expose a controller's functionality.

LabVIEW displays two windows: the front panel window and the block diagram window. The front panel or user interface appears with a gray background and is used to display controls and indicators.

The title bar indicates that this window is the front panel for the blank VI. However, the block diagram appears with a white background and includes sub Vis and graphical code structures that control the front panel objects.

Getting start was adding controls to the front panel. Controls on the front panel provide a way to input and output data through the use of controls and indictors to the block diagram of the VI. After that, adding an ActiveX control to the front panel. LabVIEW provides many standard controls and also has the ability to host third party controls through mechanisms such as ActiveX.

APT software was exposed through ActiveX to allow author to incorporate hardware control through their own custom applications. In LabVIEW the MGMotor control represents the ActiveX control used to interface with motor controller type hardware shown in Figure 3.21.

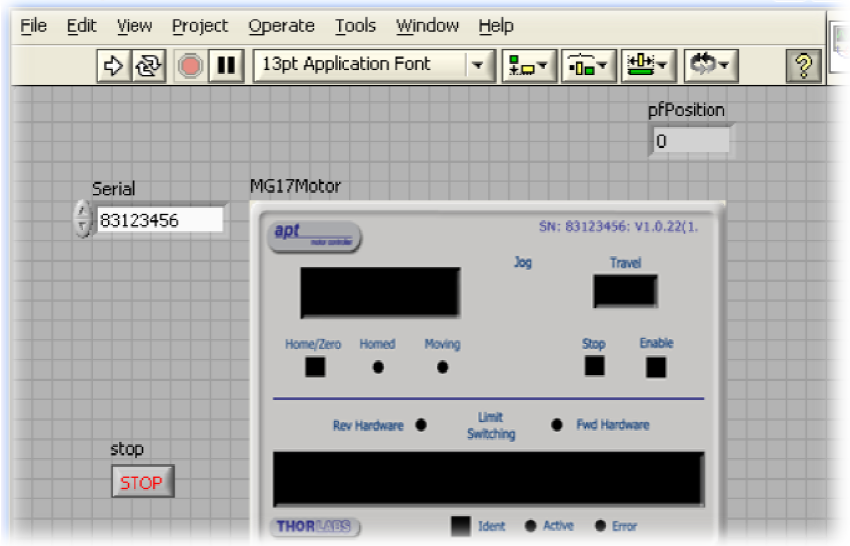

Figure 3.21: Interface front panel with Motor Controller

After complete control front panel, the continuous part was wiring objects on the block diagram. Interconnect the objects with graphical code within the block diagram to make use of the controls on the front panel.

The next part was setting an ActiveX property by Properties of the APT control objects can be set through code in the block diagram and calling an ActiveX method.

Methods of the APT control object can be called within the block diagram. Then, pass parameters to an ActiveX method. ActiveX methods can have both input and output parameters and a return parameter. Speed Controlling can't be avoided.

Although not completely necessary to ensure correct VI execution, it's good programming practice in LabVIEW to limit code execution speed where possible.

This was a good for program execution speed can be reduced without affecting the program functionality. Within the while loop a short delay to hold execution would ensure that the CPU and APT system are not over burdened with unnecessary processing. A time delay VI can be used to achieve this. The result VI was shown in Figure 3.22.

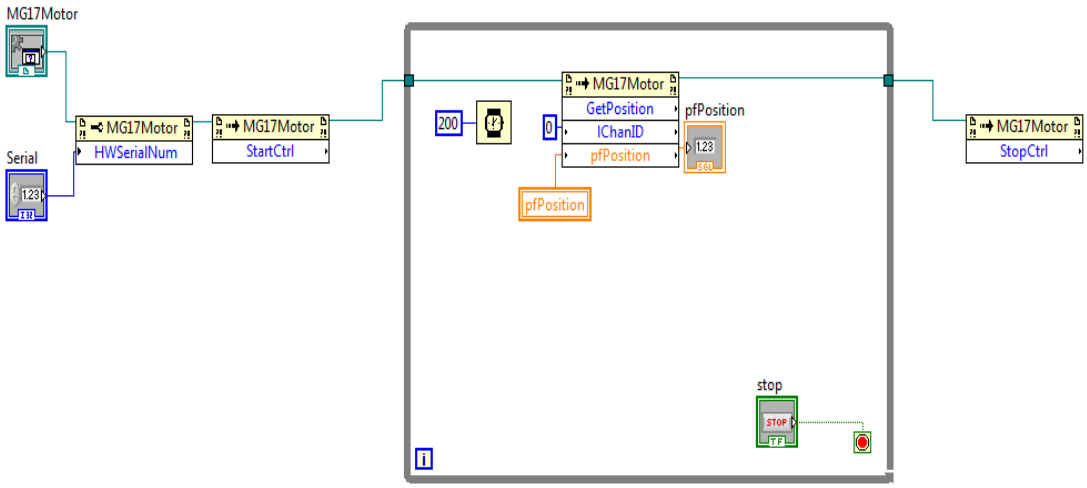

Figure 3.22: Block Diagram of Motor Controller

3.2.6.3 Controller for Aligner

Other than using software to control the aligner, author also can using the control the aligner by the manual control shown in Figure 3.23.

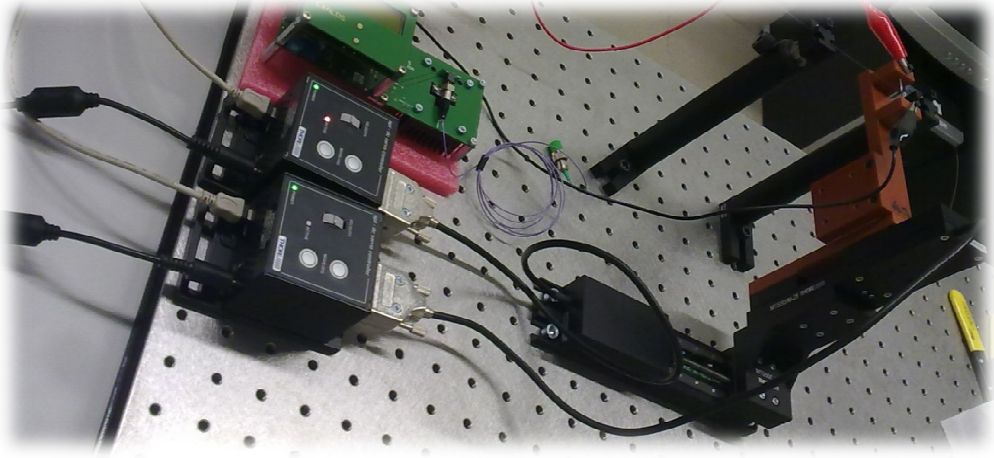

Figure 3.23: Manual Controller

3.2.7 SFG-830

The SFG-830 Series Arbitrary Function Generator is one of the most versatile and highly qualitative signal generators utilizing DDS techniques. It is not only offer the standard generator functions but also provides accurate modulations, sweep, and arbitrary waveform generation.

3.2.7.1 SFG-830 within ARB

The editing software, ARB shown in Figure 3.24 allows professional users to obtain, edit, or create frequency and amplitude characteristics as desired through RS-232C interface. The SFG-830 provide for generating arbitrary waveforms in this project for electric arching system driver.

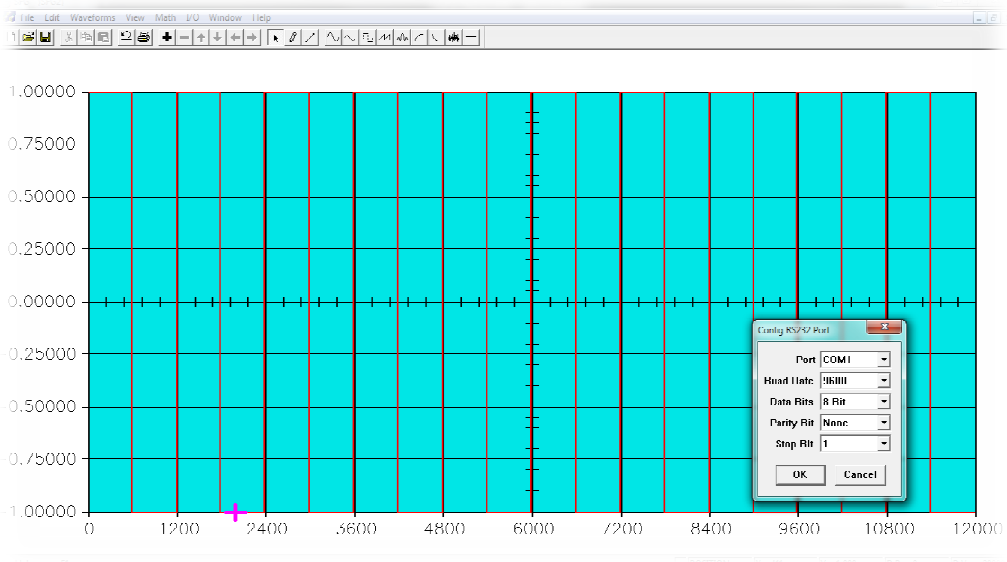

Figure 3.24: SFG-830 Using ARB Editing Software

The ARB software working well with the SFG-830 function generator while the input was creates.

3.2.7.2 SFG-830 within LabVIEW

Overall the front panel window and the block diagram were created shown in Figure 3.25 and Figure 3.26. The front panel window shown that author can set the waveform type, frequency, amplitude for the project. Before setting up the user must define the VISA resource with the function generator by using RS-232C interface included I/O, bound rate, data bits and so on.

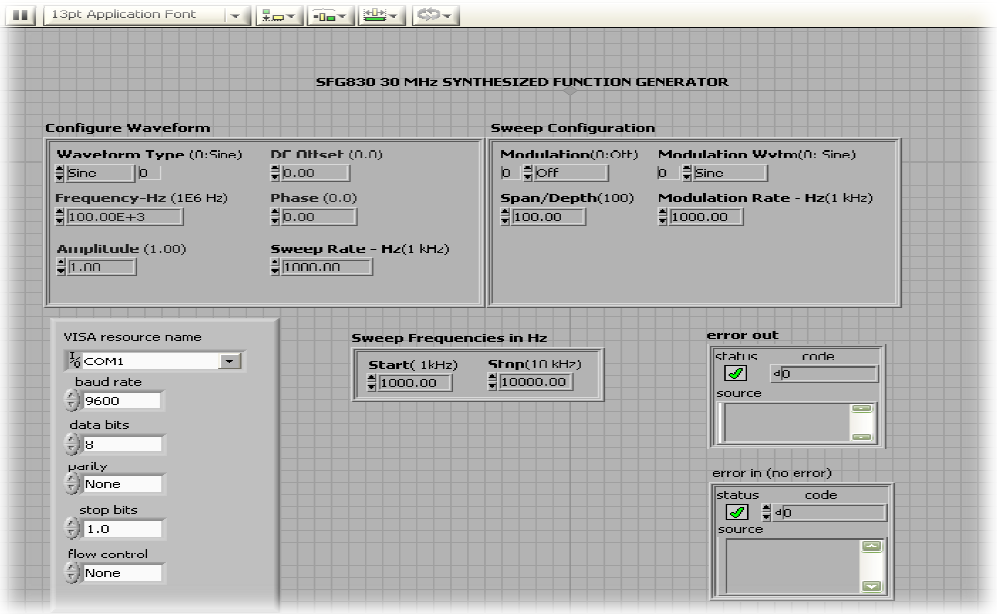

Figure 3.25: Front Panel Window of SFG-830 Function Generator

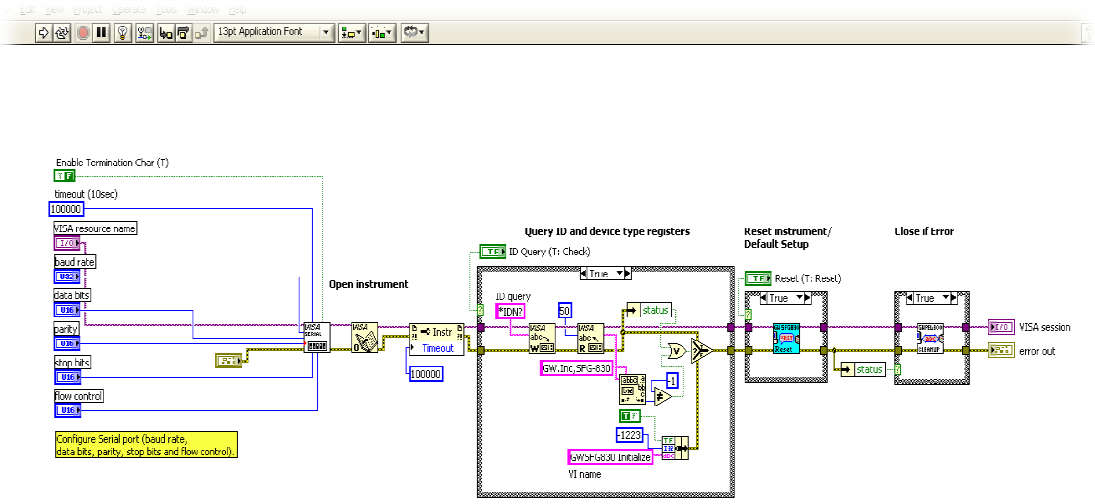

Figure 3.26: Block Diagram of SFG-830 Function Generator

3.2.8 Connectorization and Polishing Optical Fiber

Connectorization and polishing optical fiber cannot be avoided during the project execution. Author was a little experience with optical fiber. A lot of tools author was never using before to connect the optical fiber and polishing optical fiber.

3.2.8.1 Fiber Optic Cable Assembly Process Details

Flow chart shown in Figure 3.27 below was describing details about the fiber optic cable assembly process.

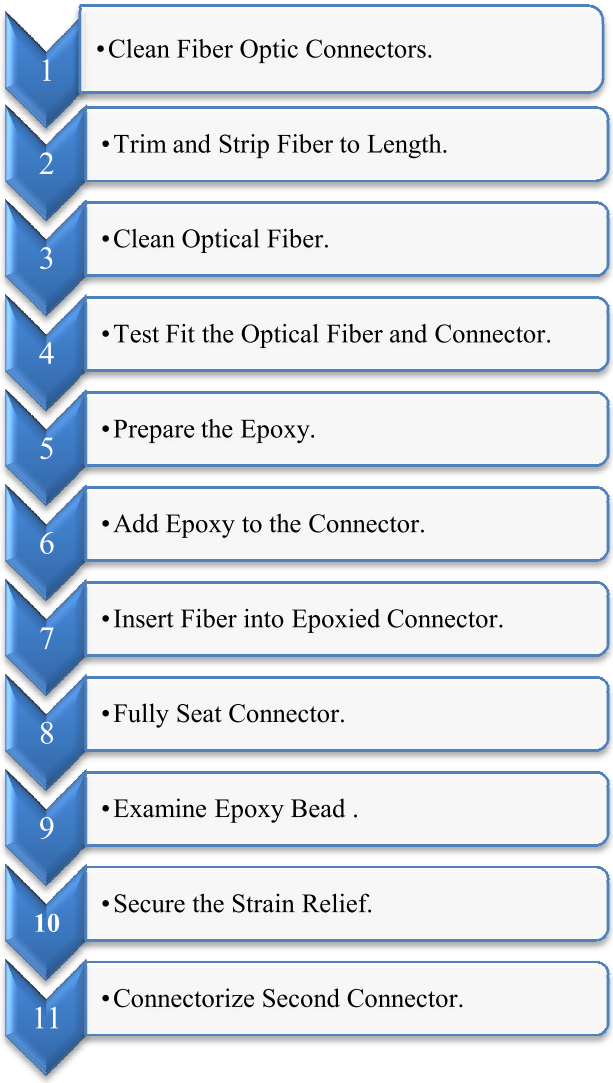

Figure 3.27: Fiber Optic Cable Assembly Process Flow Chart

Fiber connectorization begins with selecting an optical fiber and connector compatible with author's project. The optical fiber and connector are chosen, several standard and fiber and connector specific tools are required for this process assembly.

An optical fiber shown at Figure 3.28 that has been connectorized using an FC connector was shown in Figure 3.29 below.

Figure 3.28: Optical Fiber

Figure 3.29: FC Connector

The fiber optic connectors fill with enough isopropyl alcohol to completely cover the connector. After that, the connector was removed and place on a clean and dry surface.

After the connectors have completely clean, the ferrule was inspected to verify the capillary, which holds the optical fiber, was clear and free of debris. A light source used to facilitate inspection of the ferrule. Light should be clearly visible at the front of the ferrule when the light source was placed at the backside of the connector.

The optical fiber needs to be trimmed and stripped so that approximately 10 mm of stripped fiber protrudes from fiber optic connector. The total length of the optical fiber was controlled to allow proper assembly at both ends of the cable.

The actual fiber length varies depending on the individual connector manufacturer. The amount of coating was adjusted to be stripped by setting the stripper slider bar, and then the scale on the right handle allows a prescribed length of fiber to be stripped.

After the fiber was stripped, the material was removed by gently wiping the fiber with a moistened with reagent grade isopropyl alcohol. Debris left on the optical fiber was preventing proper insertion of the fiber into the ferrule.

Next, the optical fiber and connector would be tested to ensure that the fiber fits into the connector and the length of exposed fiber was sufficient for connectorization.

After the solvent has evaporated from the fiber, the stripped fiber was slipped into the back end of the connector. The connector as the fiber was rotated gently pushed through the ferrule.

Epoxy shown in Figure 3.30 was used on silica fiber. Epoxy has a working life of about 30 minutes and does not require a curing oven.

Figure 3.30: Epoxy

The epoxy was tipped to the connector body and also through the connector ferrule until a small bead shown in Figure 3.31 below appears on the outside face of the connector ferrule. After that, the connector was pushed onto the fiber while slowly rotating the connector. A small amount of epoxy was added where the crimp sleeve meets the tubing.

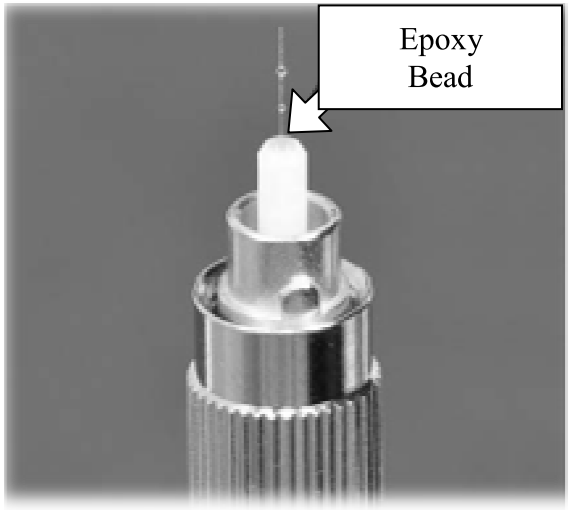

Figure 3.31: Epoxy Bead

The entire step was repeated to connectorize a second connector.

3.2.8.2 Fiber Polishing Assembly Process Details

Flow chart shown in Figure 3.32 below was describing details about the fiber polishing assembly process.

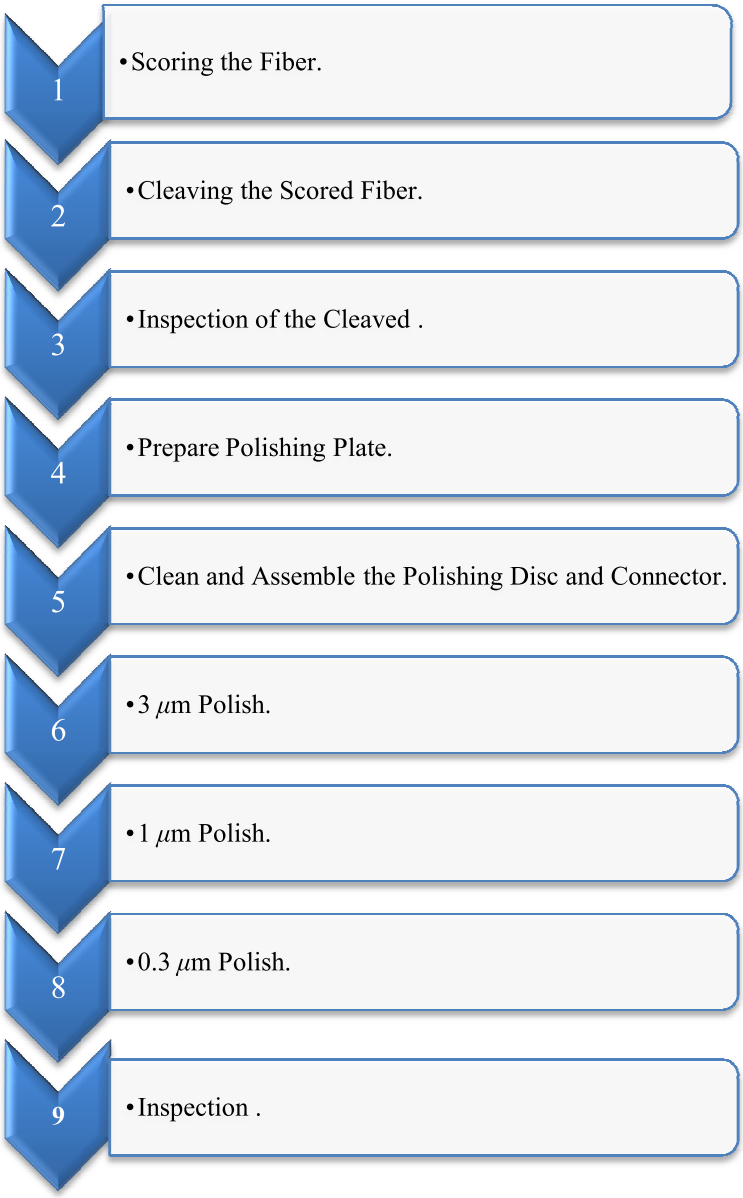

Figure 3.32: Fiber Polishing Assembly Process Flow Chart

After an optic fiber has been connectorized, the exposed fiber at the connector has been cleaved and polished to provide a low light loss connection.

In Figure 3.33 shown that a fiber scribe was used to score the fiber above the epoxy bead. The scribe was made contact with the fiber about one fiber diameter above the epoxy.

Figure 3.33: Scoring the Optical Fiber

After scoring the optical fiber, the surface of the glass polishing plate was cleaned with a lint free towel moistened with isopropyl alcohol. Then, the connector was pulled back until the fiber tip was recessed in the polishing disc.

Polishing steps were performed using 3.0 μm, following 1.0 μm and finally 0.3 μm polishing film shown in Figure 3.34. After completed the entire steps, the result in a finer polish than that achieved from the 1 μm polish and result in lower light losses.

Figure 3.34: Polishing Steps

After polishing, the connector was removed from the polishing disc and the connector ferrule was cleaned with isopropyl alcohol.

The optical fiber was completed develop shown in Figure 3.35 below.

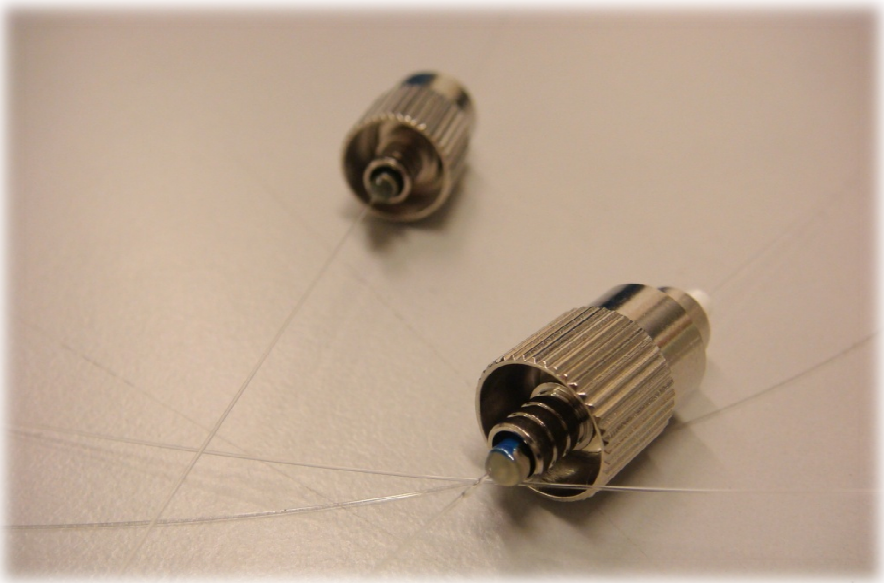

Figure 3.35: Overview Optical Fiber with FC Connector

3.2.9 SLED Driver Board EDB5080

The EBD5080 shown in Figure 3.36 is a high performance analog driver board that consists of a multi layer PCB board with a multi pin connector to which adapter boards can be connected supporting various types of optical modules.

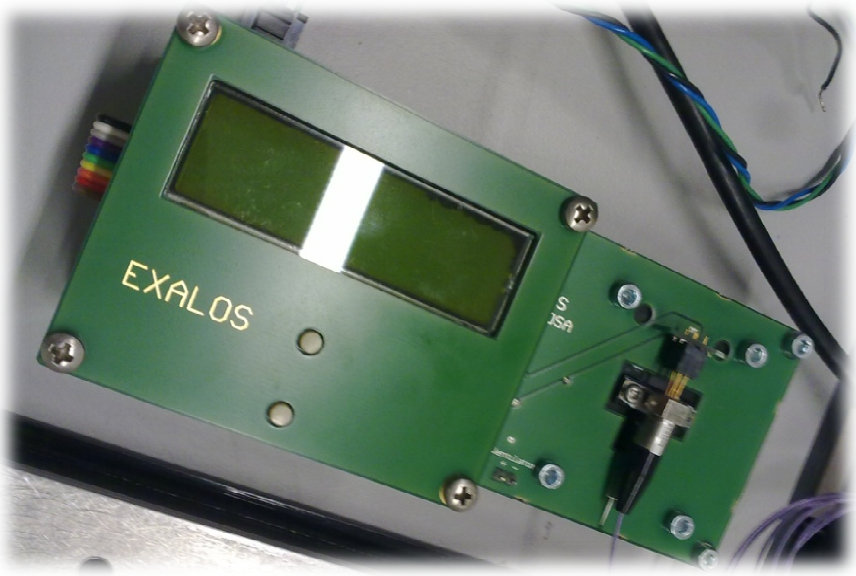

Figure 3.36: SLED Driver Board EDB5080

The multi layer PCB design with shielding ground layers allows for the coexistence of a highly efficient switched mode temperature controller (TEC) with a low noise linear super luminescent light emitting diode (SLED) drive current controller in a compact form factor with the size of a credit card.

Furthermore, the multi layer PCB design features a sophisticated heat spreading thermal design that reduces hot spots, which is the basis for stable operation at high ambient temperatures.

3.2.9.1 Operating EDB5080

Author using EDB5080 as a broadband sources provided a stable supply voltage within 5 V was applied with the correct polarity and to set the current

limit 4 A. The EBD5080 was not sensitive to noise of the supply voltage as it features various filter networks and ground decoupling stages as well as a spike and brown out detector.

The TEC was working while power supply voltage was applied to the board. The TEC is a high performance switched mode controller that was working at an internal frequency of 1 MHz. It's taking a few seconds after turn on of the board for the TEC to stabilize the SLED temperature.

The SLED was enabled and the optical power was turned on either by turning the code switch. It's enabled first power up all OpAmps of the driver stage before the optical power was turned on after a built in time delay. The turn on sequence was operated the driver board even when the power supply was hot plugged though the SLED was enabled. This means that the SLED was enabled with the drive current was set to the maximum level.

Furthermore, the driver board was generated a current ramp of several milliseconds at turn on to avoid optical power overshoots. The time delay for the turn on was depends on the SLED drive current. The SLED current level was adjusted through the potentiometer using a screw driver stage at Figure 3.37 below.

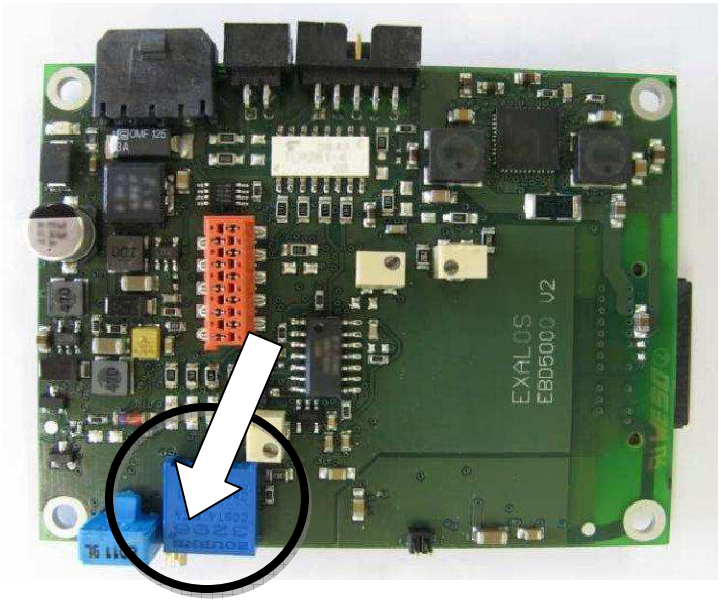

Figure 3.37: SLED Current Adjusted through Potentiometer

3.2.10 Spectrometer SM242

The SM242 is a new compact, pre-configured design CCD Spectrometer for use with a PC. Based on SP's special optical bench design, it supports many different applications where spectral or color measurements are required, including high dynamic range applications.

The SM242 can accept light directly through its built-in slit or via optical fiber. A removable faceplate allows the use of FC, and custom fiber connectors. This faceplate also allows direct attachment to dedicated systems and a number of SMX Accessories. The durable aluminum housing that encloses the SM242 provides stable optical bench operation over a wide range of temperatures.

The array driver electronics have been designed for highly sensitive yet stable operation. This array allows up to 850 *n*m measurement window from 200 *n*m to 1050 *n*m. The design of the SM242 shown in Figure 3.38 allows use of custom arrays for special applications, including photodiode assemblies and alternative CCD arrays.

Author using this device to detect the signal wavelength transmit from SLED driver board.

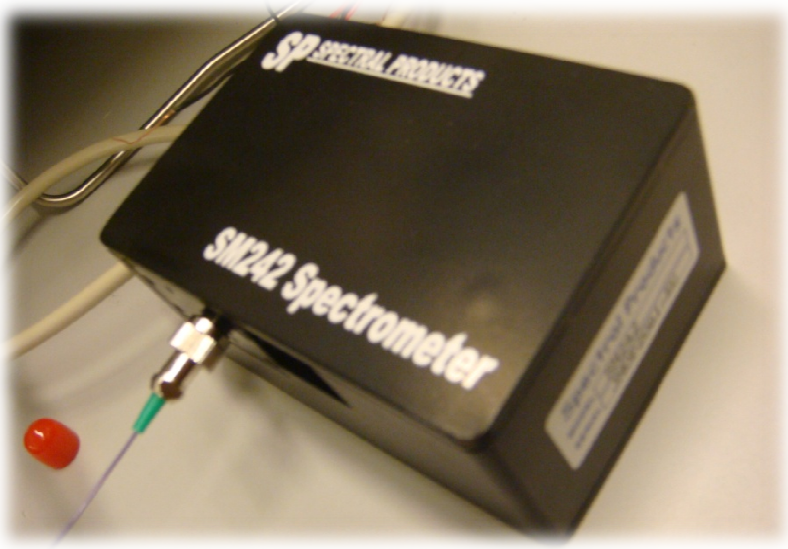

Figure 3.38: Spectrometer SM242

3.2.10.1 SM32ProForUSB

SM32Pro is a Windows based operating software designed for use with SP SM series spectrometers. SM32Pro is a true 32-bit application and optimized for SM spectrometer operation control, data acquisition, data manipulation, graphic display, and other features.

The main screen shown in Figure 3.39 consists of a menu bar, command buttons bar, cursor value and timeline recording display area, graph control buttons bar, project and sample information area, status display area, quick access controls, and a graphic display area.

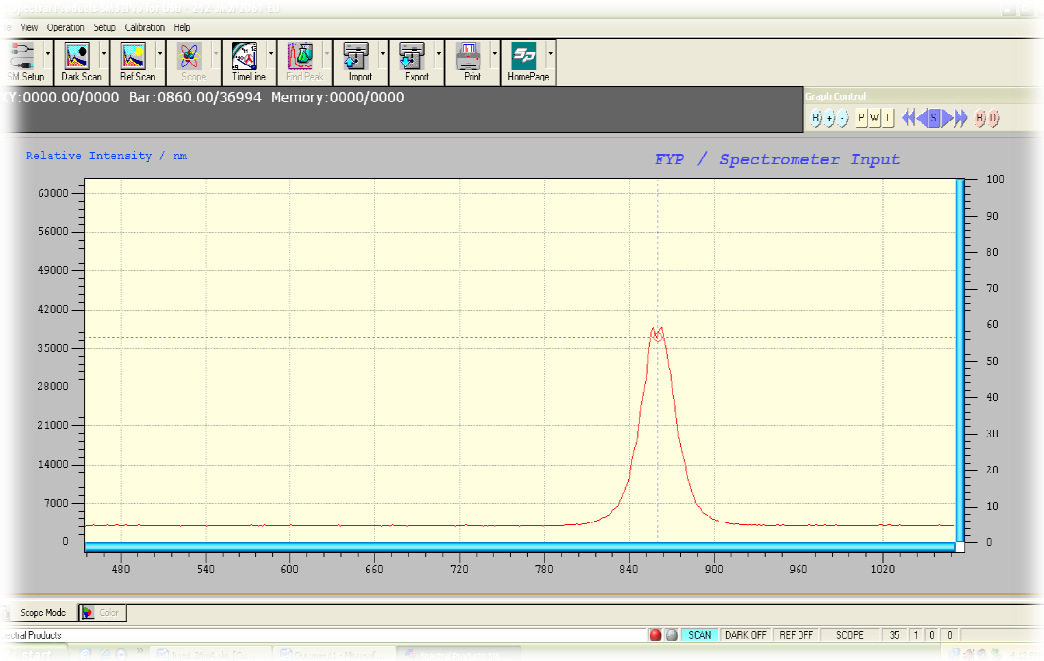

Figure 3.39: SM32Pro Operating Software

The graphic display chart consists of two Y scales as well as an X-axis. The Y-axis on the left displays a relative intensity scale in A/D counts in Scope mode while the right Y-axis is defaulted to percentage.

When in Scope mode, the X-axis display is in pixel number or in wavelength number. The maximum pixel number will display the desired wavelength range.

3.3 Overview of the Project

Overall of this project whole system of the fabrication with holding fiber optic cable with spark gap to grating fiber optic cable and using graphical programming, LabVIEW Software to control the aligner to align the fiber optic cable and control the function generator to create a signal to an electric arcing driver circuit to generate spark to grading a fiber optic cable while the system in progress.

Besides that, author was developed connectorization and polishing optical fiber to contribute this project. SLED driver board was used as broadband sources to transmit a wavelength pass through optical fiber and spectrometer was accept the light then graphic display at specific operating software.

The overview of author's project was shown in Figure 3.40 below.

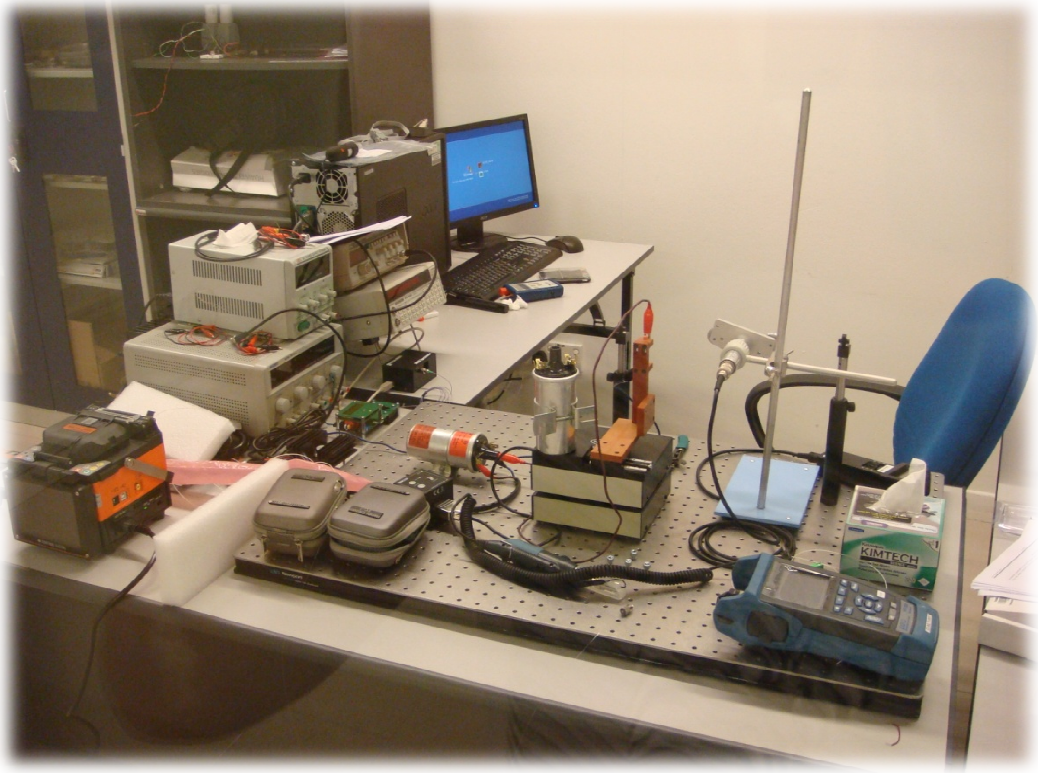

Figure 3.40: Overview of the Whole Project

CHAPTER 4

RESULT AND DISCUSSION

4.1 Testing and Measurement

The digital oscilloscope was used as a measurement tool for the electric arching driver. Besides that, the author was testing the ignition coil before connect to driver circuit. Other than that, the output power of the spark generated by ignition coil has been testing too.

Besides that, the SFG-830 function generator was generated a signal for the electric arching driver. The frequency was set either by ARB software or manual button on the function generator interface. Author's project was using LabVIEW software to control the aligner while fiber grating by electric arcing progressing.

Other than that, author was testing optical fiber connector by using multifunction loss tester. After the final inspection, author was measuring optical fiber cable by using optical power meter for losses and SM32ProForUSB for wavelength form broadband sources.

4.1.1 Testing and Measurement Electric Arcing Driver Circuit

Author was testing the electric arcing driver circuit in breadboard before developing the PCB board. First, the function generator was set to square waveform and connected to BFY51 transistor with a setting approximate 500 *m*Hz

which depend on the period of the project needed. The probe of the oscilloscope has been connected to the output of electric arcing circuit without connected the ignition coil. Then, turn on the power supply with 12 VDC. Figure 4.1 was shown that how was connected and method to measure the electric arcing driver circuit.

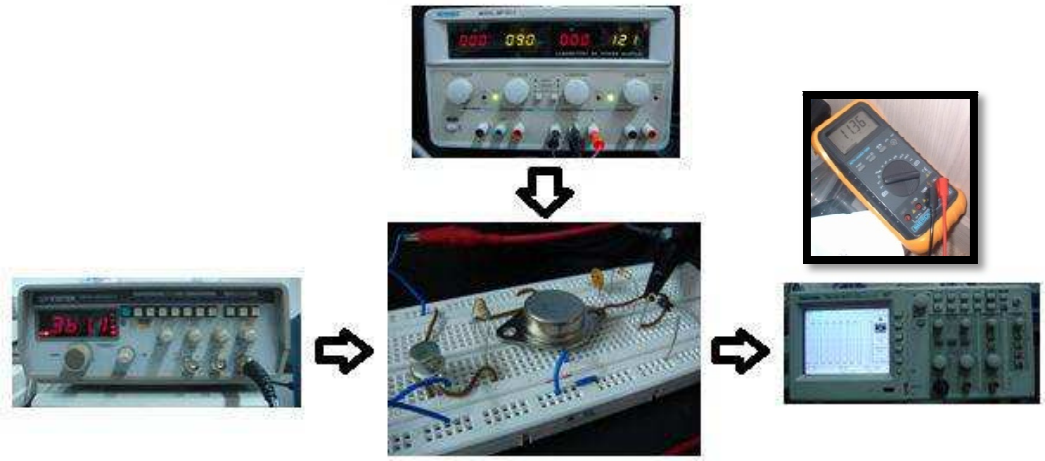

Figure 4.1: Measurement of Electric Arcing Driver Circuit

4.1.1.1 Output Waveform

The oscilloscope was primarily a voltage measuring device so using it to measure the voltage output of the electric arcing driver circuit. The waveform was shown the circuit working well. When the frequency was increase, the output wavelength will decrease; mean that the output voltage was generated quickly. Figure 4.2 was shown that the output waveform of the electric arcing circuit.

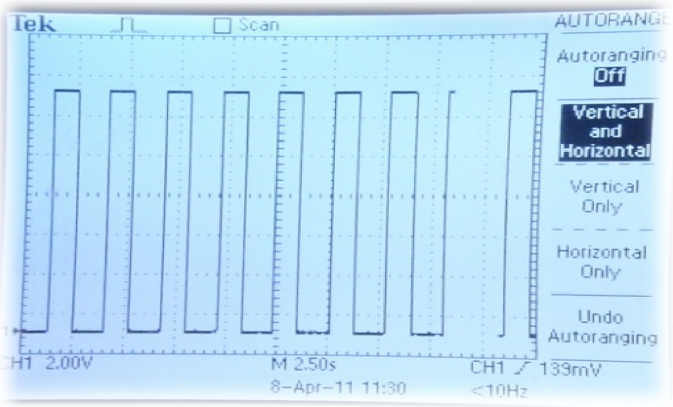

Figure 4.2: Output Waveform

4.1.1.2 Output Voltage

Another measurement has been done by using multimeter. The multimeter was connected to the electric arcing driver circuit output to measure the output voltage.

While high frequency signals were pass through the driver and power up the transistor. Therefore, the output voltage of the electric arcing driver was getting approximate 12 V.

Figure 4.3: Output Voltage

4.1.2 Testing Ignition Coil and Measuring Spark

Before the author try connect the ignition coil to the electric arcing driver circuit. Some testing was done for checking the ignition coil. The schematic diagram shown at Figure 4.4 how the author test the ignition coil.

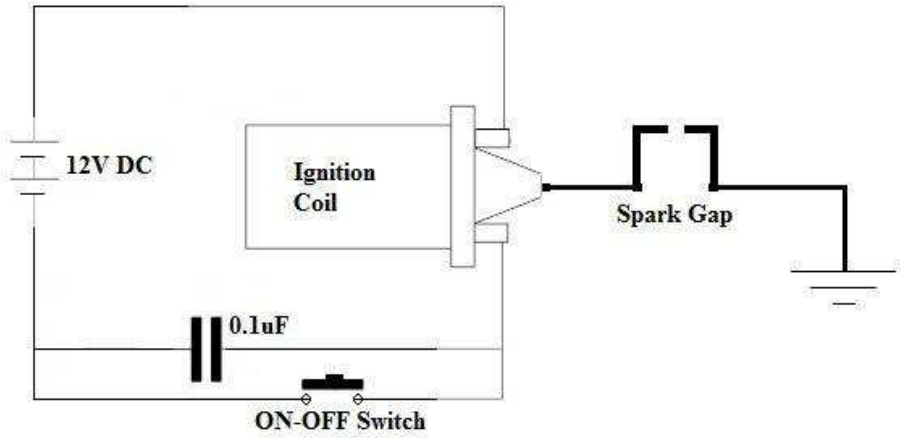

Figure 4.4: Testing Ignition Coil Schematic Diagram

When the switch was connected, circuit allows current to flow into one of the primary terminals to the primary coil. In this ignition system shown in Figure 4.5 direct current was used, because the idea was not to create steady, continuous induction, but one single, dramatic induction from a sudden collapse of a magnetic field.

As current flows to the primary coil, an increasingly large magnetic field builds up around it as well as around the secondary coil housed inside.

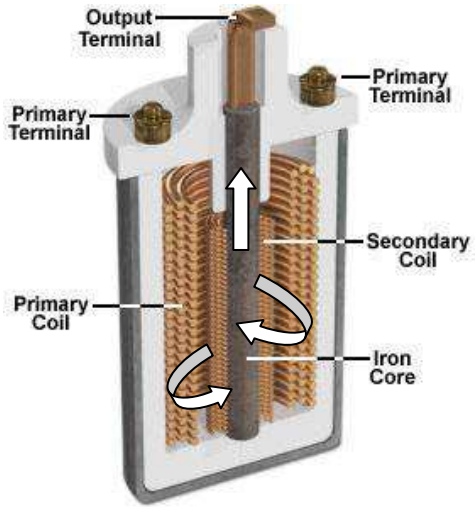

Figure 4.5: Ignition Coil System

If switch off the current, the field suddenly collapses, and this rapid change induces a surge of current in the secondary coil, which streams out the high voltage output terminal and was enough to jump the spark gap in the circuit. The spark was generated by ignition coil as shown in Figure 4.6.

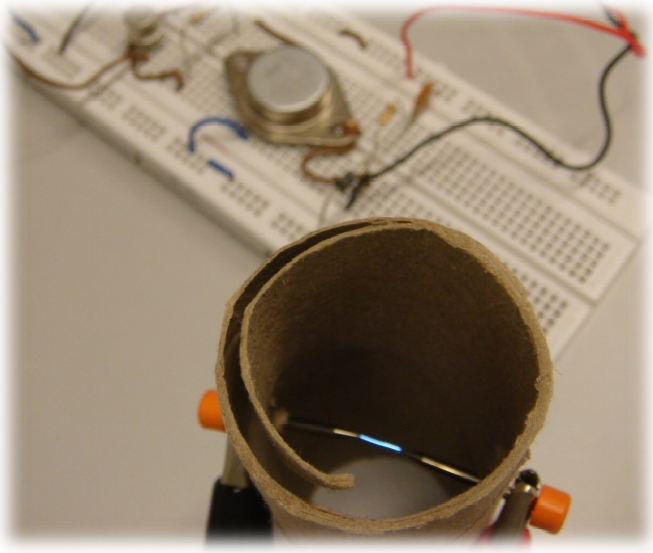

Figure 4.6: Spark Generated by Ignition Coil

There was a problem with this scenario. The collapsing field also induces a lesser surge in the primary coil and creating unwanted surge of electricity traveling back through one of the primary terminals toward the switch. To keep that surge from reaching the switch, a capacitor and resistor was inserted in the electric arching driver circuit. The function of this capacitor and resistor in ignition systems function as safely absorbs the back EMF.

4.1.3 Testing and Measurement Electric Arcing Driver Circuit after Developed in PCB

Author was testing the electric arcing driver circuit after developing the PCB board shown in Figure 4.7. The results were similar as what author gets from previous testing result.

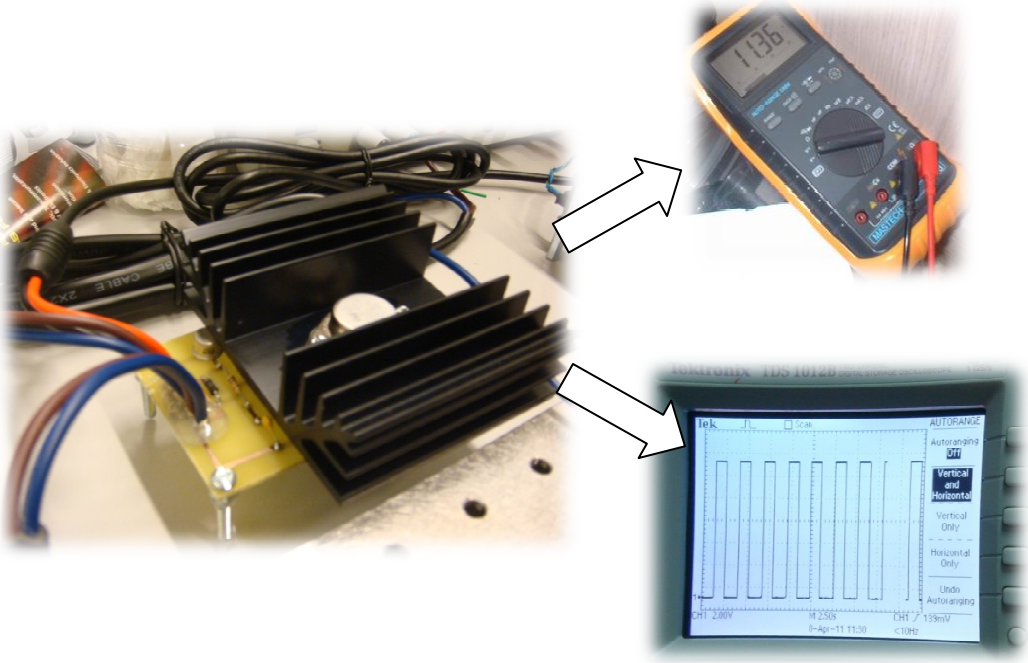

Figure 4.7: Measurement Electric Arcing Driver Circuit after Develop in PCB

4.1.4 Testing and Measuring Spark after Developed in PCB

After developed the electric arching system driver to PCB, author notice that the electric spark generate by the ignition coil become strong compare on breadboard. The electric spark was shown in Figure 4.8 below.

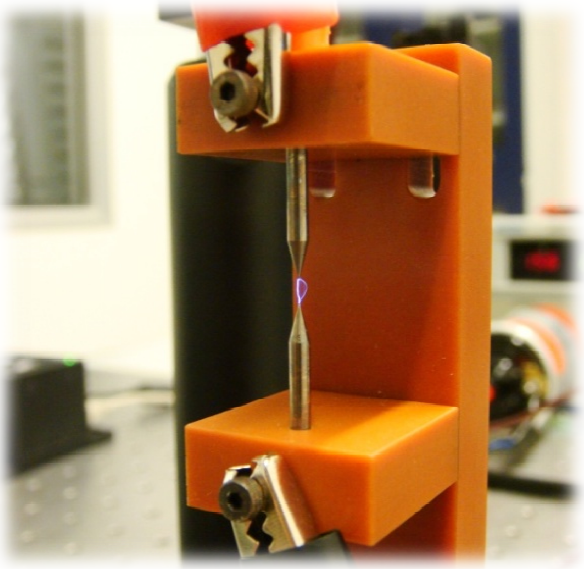

Figure 4.8: Electric Spark

The measurement of multimeter shown the output voltage of electric spark generated by ignition coil was larger than 100 V.

4.2 Running a Virtual Instrument (VI) with APT by LabVIEW

The motor controller VI can be run from either the block diagram or the front panel. It is preferential in most cases to run from the front panel as all the visible controls were located within this window.

The VI communicating was run with a simulated DC motor controller (TDC001) with a serial number of the motor shown in Figure 4.9.

Figure 4.9: VI with Live Data

Within the LabVIEW development environment it's possible to stop execution by pressing the stop button on the menu toll bar. It noted that in stopping the VI in this manner does not stop communication to the APT controls and any such disconnection of the equipment will result in an error dialogue.

4.2.1 Testing Electric Arcing Driver and Running VI with APT Parallel

First, the electric arcing driver connected to ignition coil. The SFG-830 function generator was set to square waveform and connected electric arching driver with a setting 500 *m*Hz. Then, turn on the power supply with 12 VDC with current 2 A. The electrical arching driver was start generated a spark grating fiber optic and motor aligner also start moving. While the ignition coil generated one spark to output, the aligner will move a constant short distance and another spark will generate out again. The cycle of the aligner operation was set by author.

4.3 Running SFG-830 within LabVIEW

Author was facing some error problem synchronize LabVIEW software with the SFG-830 function generator shown in Figure 4.10.

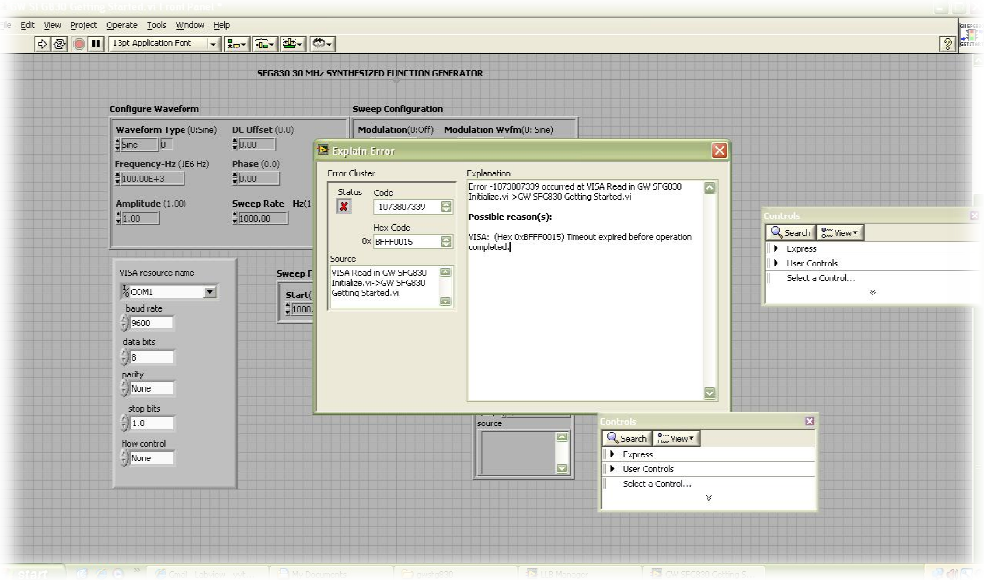

Figure 4.10: Error Problem Synchronize LabVIEW with SFG-830

Author was searching out the problem as know by using RS-232 to synchronize with SFG-830 function generator got some blocking problem because the hardware cannot recognize the data sent by computer. Other than that, RS-232 was slow and speeds as the distance increases owing to capacitance effects.

According by person who profession in LabVIEW field, it should add on software between both of them to synchronize each other. So, author recommendation was using general purpose interface bus (GPIB) in future development because GPIB also known as an IEEE-488 standard parallel interface used for attaching sensors and programmable instruments to a computer. The advantages of GPIB were fast and data transfer rate with suitable Windows software almost reach 200 Kilobytes per second. It also can connect 14 devices to one GPIB. However, add on GPIB adaptor card needed in computer.

4.4 Testing Optical Fiber with Connector

After polishing, the connector was removed from the polishing disc and the connector ferrule was cleans with isopropyl alcohol. The multifunction loss tester shown in Figure 4.11 was used to doing final inspection for optical fiber connector.

Figure 4.11: Multifunction Loss Tester

The multifunction loss tester output result, magnified views of optical fiber connector shown in Figure 4.12 justify that the connector end surface is free of epoxy. The fiber was flushed with the end of the connector ferrule. Other than that,

there were no heavy scratches through the core of the fiber. However, the majority of the area of the fiber was free of all visible scratches or defects.

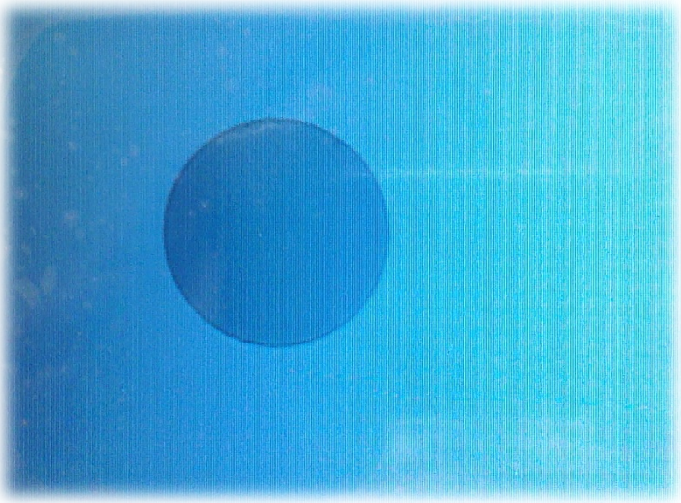

Figure 4.12: Magnified Views of Optical Fiber Connector

4.4.1 Measuring Optical Fiber Cable by Using Optical Power Meter

Before connect with the optical fiber cable, author was using optical power meter to measure output power of SLED driver board shown in Figure 4.13. When the SLED current set to 23 *m*A, the optical power meter value was -16.1 dB*m*.

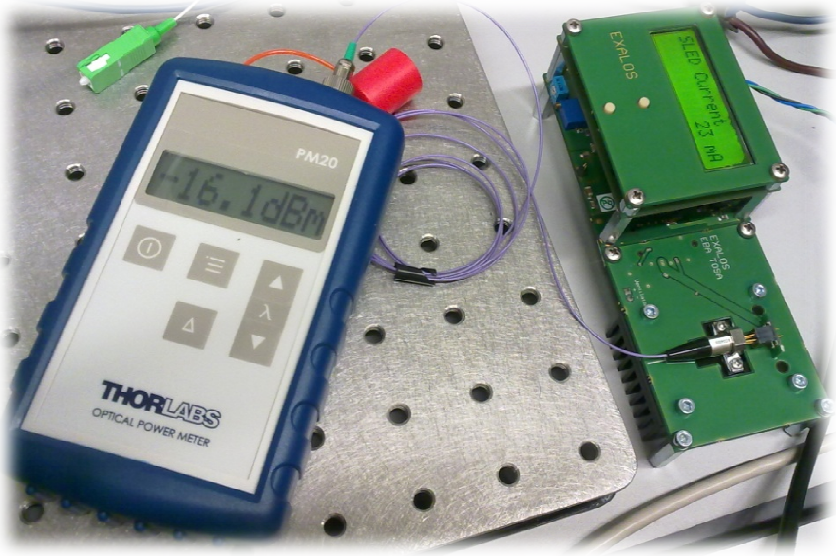

Figure 4.13: Output Power of SLED Driver Board

After connected with the optical fiber cable, author was notice that the output power value was change from -16.1 dB*m* to -17.3 dB*m* shown in Figure 4.14. There was totally losing 1.2 dB*m* after pass through optical fiber cable. The output result was acceptable.

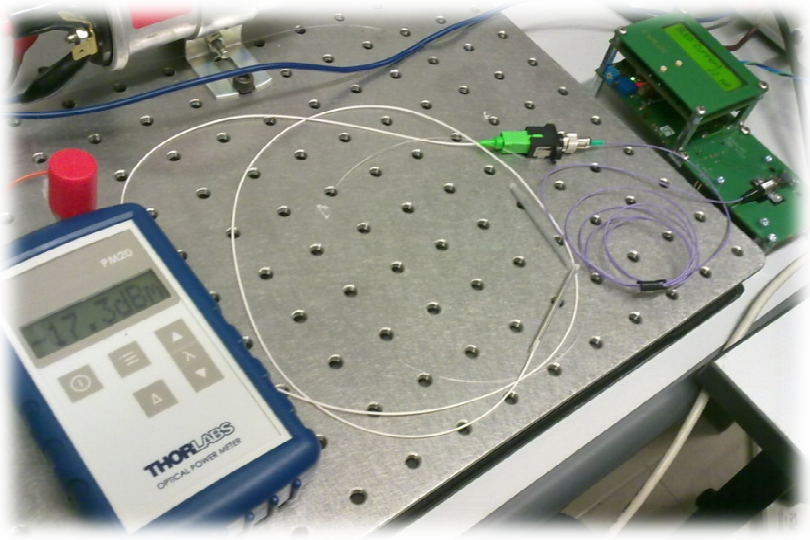

Figure 4.14: Output Power after Pass through Optical Fiber Cable

4.4.2 Measuring Optical Fiber Cable by Using SM32ProForUSB

Other than using optical power meter to measure the losses, author also using the spectrometer to measure the output wavelength of SLED driver board.

The graphic display chart consists of two Y scales as well as an X-axis shown in Figure 4.15.

According to Figure 4.15, the Y-axis on the left displays a relative intensity scale in A/D counts in Scope mode that was approximate 64810 nm while the right Y-axis was defaulted to percentage. When in Scope mode, the X-axis display was in pixel number or in wavelength number as 860.

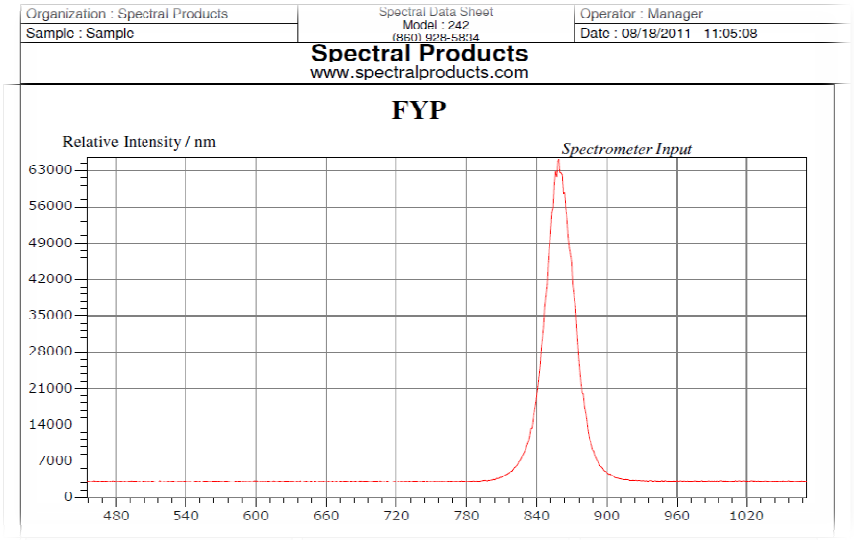

Figure 4.15: Output Wavelength of SLED Driver Board

However, the output wavelength after optical fiber cable was shown in Figure 4.16.

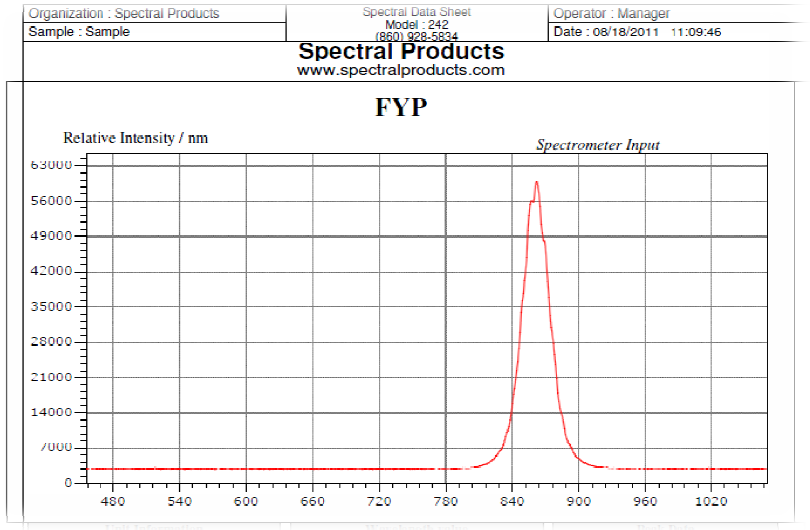

Figure 4.16: Output Wavelength after Pass through Optical Fiber Cable

According to Figure 4.16, the Y-axis on the left displays a relative intensity scale in A/D counts in Scope mode that was approximate 60000 nm while the right Y-axis was defaulted to percentage. When in Scope mode, the X-axis display was in pixel number or in wavelength number as 860 same as default. This was normal because the optical fiber cable have no modulated refractive index because author never done grating.

4.5 Testing Optical Fiber after Grating

After measuring optical fiber cable by using SM32ProForUSB and the original data was collected, author was testing the optical fiber with grating for a few setting after grating. The frequency to generate a clock signal for the electric arching driver circuit was set to 500 Hz and the amplitude of the function generator was set to 10 V_{pp} to power up the ignition coil. Figure 4.17 shown the grating process of the electric spark generate by the ignition coil.

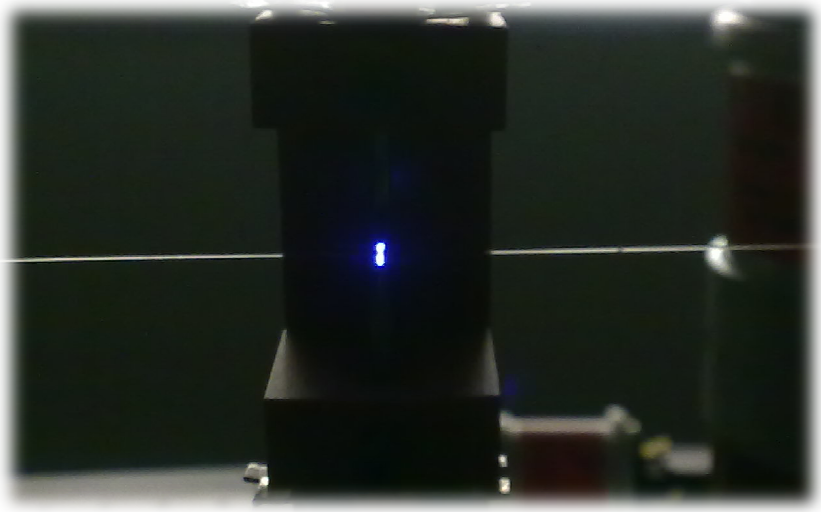

Figure 4.17: Grating Process Using Electric Spark

4.5.1 Grating Data

Two types of setting was been used for test the grating process, that was 4 seconds with 20 gratings and 1 minute with 10 gratings compare with original before grating. The grating data wavelength range starting from 455 - 1071 *n*m was shown in Table 4.18.

Wavelength (*n*m)	Original before grating intensity(Counts)	4 seconds with 20 gratings intensity(Counts)	1 minutes with 10 gratings intensity(Counts)
455 - 800	≈ 3262	≈ 3266	≈ 3229
801 - 817	≈ 3858	≈ 3839	≈ 3661
818 - 828	≈ 5126	≈ 4967	≈ 4409
829 - 839	≈ 10097	≈ 10199	≈ 8093
840-858	≈ 23195	≈ 22700	≈ 16960
859	≈ 35489	≈ 34964	≈ 25973
861 - 872	≈ 21419	≈ 21213	≈ 16387
873 - 879	≈ 11165	≈ 11023	≈ 8619
880 - 890	≈ 5483	≈ 5386	≈ 4877
897 - 1071	≈ 3116	≈ 3234	≈ 3195

Table 4.18: Grating Data for Two Types of Setting

After the grating data was collected and the graph was plotted in Figure 4.19 below.

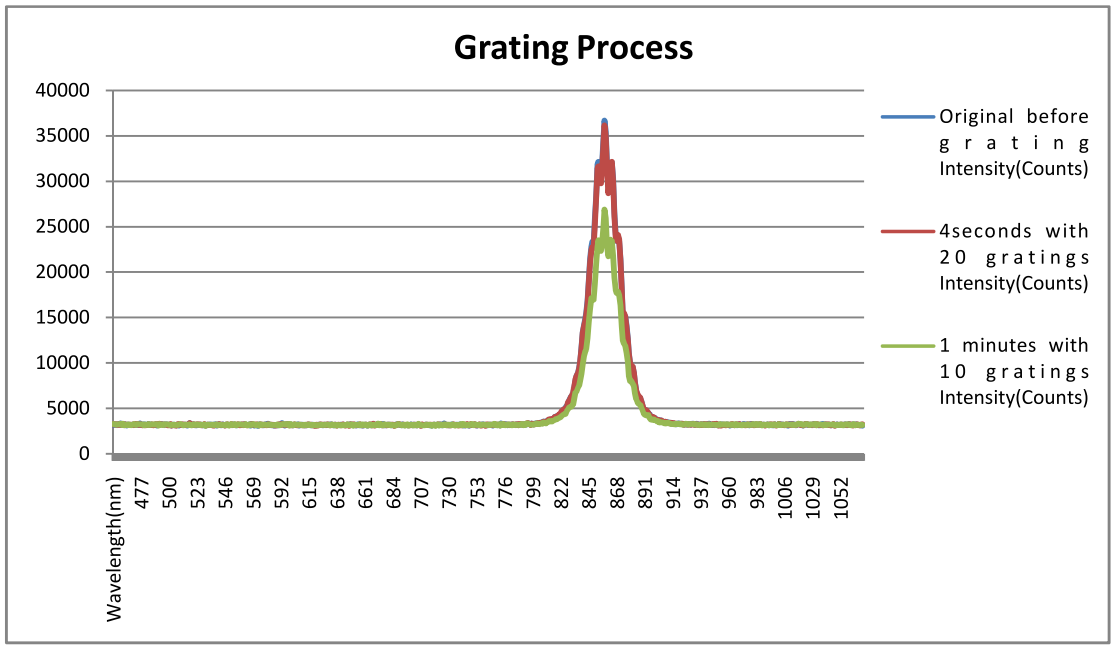

Figure 4.19: Grating Data Before and After Grating

The line in Figure 4.19 plots the wavelength spectrum written in SM32ProForUSB with author's project. In the wavelength range 455 – 1071 *n*m, it exhibits several wavelength spectrums to relative intensity scale in A/D counts in Scope mode that was approximate 40000 counts identified in the same graph. The two different after grating data with original before grating data centered to 800

*n*m and 900 *n*m by spectrometer for spectral measurements. According to graph shown in Figure 4.19, the optimum wavelength of the original before grating was approximate 35489 counts and 4 seconds with 20 gratings was approximate 34964 counts and 1 minute with 10 gratings was approximate 25973 counts. This means that the fiber cladding reduction induces modifications in the distribution of the cladding modes leading to changes in the spectral characteristics.

Based on the figure results, author can conclude that the grating period and number of gratings intensity of the fiber induces a sensitivity enhancement towards the refractive index.

The method was based on periodic melting of the fiber, while a pulling weight stretches it, thus determining a periodically tapered fiber. The grating period was mainly determined by the moving step of the aligner that was controlled by a computer and by some other factors such as arc intensity, arc duration time, and pulling weight. The fabrication setup just like what author mention at previous chapter.

CHAPTER 5

CONCLUSION AND RECOMMENDATIONS

5.1 Conclusion

Overall of this project, the author was just completed develop the electric arcing system driver for grating fiber optic and control the motor aligner by LabVIEW. A small part was synchronize the SFG-830 function generator to create a signal to an electric arcing driver while the system in progress.

During the progress on this project, author was doing a lot of research and reading article related with this project. A lot of new theory and method was learnt during doing research. Some lecture theories was applied in the project also. Author set up appliances easily because of usually using it during practical period.

Other than that, author was also facing a lot of problem doing the project and can't find out information related with the project. A lot of new theory and method was applied during doing the project while facing problem. Some theories were applied in the project also but didn't work. A lot of appliances was change because of can't synchronize with the software with hardware.

Although a lot of hardness facing during the project was progressing, author never gives up finding out the problem and solving it. On the other hand, author has leant a lot practical skills during the project because using many types of optical appliances such as broadband sources device, spectrometer, multifunction loss tester, optical power meter, DCM fusion splicer and so on.

The outcome of this project was in progressing to hit the aims and objectives.

5.2 Recommendations and Future Development

Although a lot of part of the project was completed, but still have a lot of recommendations to improve this project.

During first semester, author planning to move the electric arcing driver circuit develop in PCB board at because of breadboard was noisier not a good conductor. It does not support frequencies as high as properly and take up more physical space than the PCB. At last author was completed fabricated electric arcing driver system for grating fiber optic on PCB.

Another recommendation was install a heat sink for 2N3055 transistor to stay cool and work better. This will protect the transistors because a lot of heat was generated when the high current flows through a transistor. Author also completed install on transistor and the circuit function and working well.

Although some part future development of the project was complete improvement, but still has recommendations to improve this project. Author plans to improve the electric arcing driver to generate stronger spark. Author plans to change the 2N3055 transistor to IGBT or MOSFET. The reason was IGBT can switching times as well as low power losses however MOSFET have very fast switching characteristics as low turn on and turn off times. It would work better use in this circuit as long as it is rated for at last 5 A and 100 V.

Another recommendation was author recommendation was using general purpose interface bus replace with RS-232 in future development because GPIB used for attaching sensors and programmable instruments to a computer. The advantages of GPIB were fast and data transfer rate with suitable Windows software very high. It also can connect 14 devices to one GPIB at the same time.

Although based on the results, author can conclude that the grating period and number of gratings intensity of the fiber induces a sensitivity enhancement towards the refractive index. But author still need some research to improve the project for future development because different environment and different type of material or supplier will bring out different parameter and result.

REFERENCES

[1] E. Udd, ed., Fiber Optic Sensors: An Introduction for Engineers and Scientists, Wiley, New York, 1991.

[2] E. Udd, ed., Fiber optic sensors, Proc. SPIE, CR-44, 1992.

[3] Francis T. S. Yu, Shizhuo Yin, Optical fiber sensor, The Pennsylvania State University, University Park, Pennsylvania, 2002.

[4] Stuart (Shizhuo) Yin, Paul Ruffin, Francis T. S. Yu, Optical fiber sensor (2^{nd} ed.), Taylor & Francis Group, LLC, 2008.

[5] A. D. Kerscy, M. A. Davis, H. J. Patrick, M. LeBlanc, K. P. Koo, C. G. Askins, M. A. Putnam, and E. J. Friebeie, Fiber grating sensors, J. Lightwave Tech., 1997.

[6] Stuart (Shizhuo) Yin, Paul Ruffin, Francis T. S. Yu, Optical fiber sensor (2^{nd} ed.), Taylor & Francis Group, LLC, 2008.

[7] Francis T. S. Yu, Shizhuo Yin, Optical fiber sensor, The Pennsylvania State University, University Park, Pennsylvania, 2002.

[8] H. J. Patrick, A. D. Kersey, and F. Bucholtz, Analysis of the response of long period fiber gratings to external index of refraction, J. Light wave Tech., 1998.

[9] Z. Chen, K. S. Chiang, M. N. Ng, Y. M. Chan, and H. Ke, Bend long-period fiber gratings for sensor applications, Proc. SPIE on Advanced Photonic Sensors and Applications, Singapore, 1999.

[10] Stuart (Shizhuo) Yin, Paul Ruffin, Francis T. S. Yu, Optical fiber sensor (2^{nd} ed.), Taylor & Francis Group, LLC, 2008.

[11] Bhatia V 1999 Applications of long-period gratings to single and multi-parameter sensing Opt. Express 4.

[12] Francis T. S. Yu, Shizhuo Yin, Optical fiber sensor, The Pennsylvania State University, University Park, Pennsylvania, 2002.

[13] StephenWJames, Ralph P Tatam, Optical fiber long-period grating sensors: characteristics and application, Cranfield University, Cranfield, Bedford MK43 OAL, UK, 2003.

[14] StephenWJames, Ralph P Tatam, Optical fiber long-period grating sensors: characteristics and application, Cranfield University, Cranfield, Bedford MK43 OAL, UK, 2003.

[15] Chen K P, Herman P R, Tam R and Zhang J 2000 Rapid long-period grating formation in hydrogen loaded fiber with 157 nm F2 laser radiation Electron. Lett.

[16] Kashyap R 1999 Fibre Bragg Gratings (London: Academic).

[17] Vengsarkar A M, Lemaire P J, Judkins J B, Bhatia V, Erdogan T and Sipe J E 1996 Long-period fiber gratings as band rejection filters J. Light wave Technol.

[18] Hwang I K, Yun S H and Kim B Y 1999 Long period fiber grating based upon periodic microbends Opt. Lett.

[19] Kakarantzas G, Dimmick T E, Birks T A, Le Roux R and Russell P St J 2001 Miniature all-fiber devices based on CO2 micro structuring of tapered fibers Opt. Lett.

[20] Lin C-Y, Chern G-W andWang L A 2001 Periodical corrugated structure for forming sampled fibre Bragg grating and long-period fiber grating with tunable coupling strength J. Light wave Technol.

[21] Ye C C, James S W and Tatam R P 2000 Simultaneous temperature and bend sensing using long-period fiber gratings Opt. Lett.

[22] StephenWJames, Ralph P Tatam, Optical fiber long-period grating sensors: characteristics and application, Cranfield University, Cranfield, Bedford MK43 OAL, UK, 2003.

[23] Free encyclopedia, from Wikipedia. Ignition system. Retrieved March 27, 2011, from http://en.wikipedia.org/wiki/Ignition_system.

[24] Free encyclopedia, from Wikipedia. Electric Arc. Retrieved March 06, 2011, from http://en.wikipedia.org/wiki/Arcing.

[25] Free encyclopedia, from Wikipedia. Ignition coil. Retrieved March 06, 2011, from http://en.wikipedia.org/wiki/Ignition_coil#Tesla_coil.

[26] Free encyclopedia, from Wikipedia. Spark gaps. Retrieved March 20, 2011, from http://en.wikipedia.org/wiki/Spark_gap#Ignition_devices.

APPENDIX A: Final Year Project Gantt Chart

Finaly Year Project 2011

Task	Start	End	Duration	1/17	1/24	1/31	2/7	2/14	2/21	2/28	3/7	3/14	3/21	3/28	4/4	4/11
Briefing about Final Year Project	1/17/2011	1/24/2011	6													
Final Year Project Title Announce	1/24/2011	1/31/2011	6													
Choosing Final Year Porject Title	2/7/2011	2/8/2011	2													
Doing Reseach For The Title & Topic	1/24/2011	4/11/2011	56													
Set Up the Photonic Research Lab	2/17/2011	3/17/2011	21													
Design Electric Arcing Circuit	2/10/2011	2/20/2011	7													
Testing Electric Arcing Circuit	2/20/2011	2/27/2011	5													
Testing Fail	2/27/2011	2/28/2011	1													
Redesign Circuit	3/1/2011	3/7/2011	5													
Ignition Coil	3/1/2011	3/9/2011	7													
Testing Pass	3/1/2011	3/10/2011	8													
Found the Setting	3/1/2011	4/9/2011	29													
Prepare for FYP proposal	2/28/2011	4/15/2011	35													
Pass Up FYP Proposal	4/15/2011	4/16/2011	1													
FYP Proposal Presentation	11/17/2011	12/28/2011	30													

APPENDIX B: Final Year Project Process Flow Chart

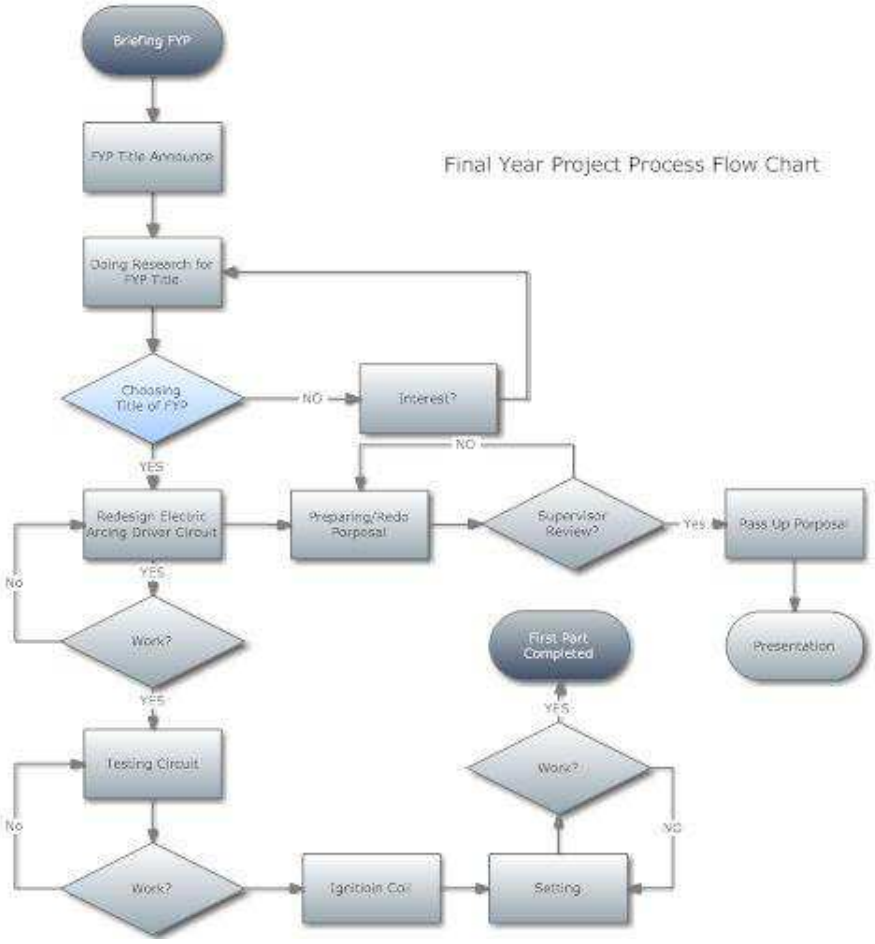

SGS-THOMSON MICROELECTRONICS

BFY50/51

MEDIUM POWER AMPLIFIER

DESCRIPTION

The BFY50 and BFY52 are silicon planar epitaxial NPN transistors in Jedec TO-39 metal case. They are intended for general purpose linear and switching applications.

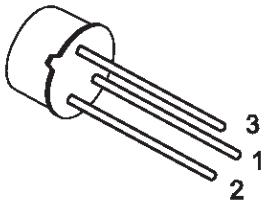

TO-39

INTERNAL SCHEMATIC DIAGRAM

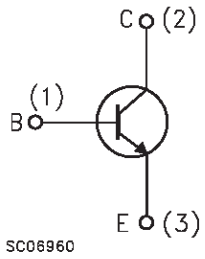

ABSOLUTE MAXIMUM RATINGS

Symbol	Parameter	Value		Unit
		BFY50	BFY51	
V_{CBO}	Collector-Base Voltage (I_E = 0)	80	60	V
V_{CEO}	Collector-Emitter Voltage (I_B = 0)	35	30	V
V_{EBO}	Emitter-Base Voltage (I_C = 0)	6		V
I_C	Collector Current	1		A
I_{CM}	Collector Peak Current (t_p < 5 ms)	1.5		A
P_{tot}	Total Dissipation at $T_{amb} \leq 25\ ^oC$ at $T_{case} \leq 25\ ^oC$	0.8 5		W W
T_{stg}	Storage Temperature	-65 to 200		^oC
T_j	Max. Operating Junction Temperature	200		^oC

THERMAL DATA

$R_{thj\text{-}case}$	Thermal Resistance Junction-Case Max	35	°C/W
$R_{thj\text{-}amb}$	Thermal Resistance Junction-Ambient Max	218	°C/W

ELECTRICAL CHARACTERISTICS (T_{case} = 25 °C unless otherwise specified)

Symbol	Parameter	Test Conditions	Min.	Typ.	Max.	Unit
I_{CBO}	Collector Cut-off Current (I_E = 0)	for **BFY50**				
		V_{CB} = 60 V			50	nA
		V_{CB} = 60 V T_{case} = 100 °C			2.5	µA
		for **BFY51**				
		V_{CB} = 40 V			50	nA
		V_{CB} = 40 V T_{case} = 100 °C			2.5	µA
I_{EBO}	Emitter Cut-off Current (I_C = 0)	V_{EB} = 5 V			50	nA
		V_{EB} = 5 V T_{case} = 100 °C			2.5	µA
$V_{(BR)CBO}$	Collector-Base Breakdown Voltage (IE = 0)	I_C = 100 µA				
		for **BFY50**	80			V
		for **BFY51**	60			V
$V_{(BR)CEO}$*	Collector-Emitter Breakdown Voltage (I_B = 0)	I_C = 30 mA				
		for **BFY50**	35			V
		for **BFY51**	30			V
$V_{(BR)EBO}$	Emitter-Base Breakdown Voltage (I_C = 0)	I_C = 100 µA	6			V
$V_{CE(sat)}$*	Collector-Emitter Saturation Voltage	I_C = 150 mA I_B = 15 mA				
		for **BFY50**		0.14	0.2	V
		for **BFY51**		0.14	0.35	V
		I_C = 1 A I_B = 0.1 A				
		for **BFY50**		0.7	1	V
		for **BFY51**		0.7	1.6	V
$V_{BE(sat)}$*	Base-Emitter Saturation Voltage	I_C = 150 mA I_B = 15 mA		0.95	1.3	V
		I_C = 1 A I_B = 0.1 A		1.5	2	V
h_{FE}*	DC Current Gain	for **BFY50**				
		I_C = 10 mA V_{CE} = 10 V	20	40		
		I_C = 150 mA V_{CE} = 10 V	30	55		
		I_C = 1A V_{CE} = 10 V	15	30		
		for **BFY51**				
		I_C = 10 mA V_{CE} = 10 V	30	55		
		I_C = 150 mA V_{CE} = 10 V	40	70		
		I_C = 1A V_{CE} = 10 V	15	40		
h_{fe}*	Small Signal Current Gain	V_{CE} = 6 V f = 1KHz				
		I_C = 1 mA				
		for **BFY50**		25		
		for **BFY51**		30		
		I_C = 10 mA				
		for **BFY50**		45		
		for **BFY51**		60		
f_T	Transition Frequency	I_C = 50 mA V_{CE} = 10 V				
		for **BFY50**	60	100		MHz
		for **BFY51**	50	110		MHz
C_{CBO}	Collector Base Capacitance	I_E = 0 V_{CB} = 10 V f = 1MHz		10		pF

* Pulsed: Pulse duration = 300 µs, duty cycle ≤ 1 %

ELECTRICAL CHARACTERISTICS (continued)

Symbol	Parameter	Test Conditions	Min.	Typ.	Max.	Unit
h_{ie}	Input Impedance	I_C = 10 mA V_{CE} = 5 V f = 1KHz for **BFY50** for **BFY51**		 180 220		 Ω Ω
h_{re}	Reverse Voltage Ratio	I_C = 10 mA V_{CE} = 5 V f = 1KHz for **BFY50** for **BFY51**		 55 70		 10^{-6} 10^{-6}
h_{oe}	Output Admittance	I_C = 10 mA V_{CE} = 5 V f = 1KHz for **BFY50** for **BFY51**		 30 35		 µS µS
t_d	Delay Time	I_C = 150 mA V_{CC} = 10 V I_{B1} = 15 mA V_{BE} = -2 V		15		ns
t_r	Rise Time	I_C = 150 mA V_{CC} = 10 V I_{B1} = 15 mA V_{BE} = -2 V		40		ns
t_s	Storage Time	I_C = 150 mA V_{CC} = 10 V I_{B1} = $-I_{B2}$ = 15 mA		300		ns
t_f	Fall Time	I_C = 150 mA V_{CC} = 10 V I_{B1} = $-I_{B2}$ = 15 mA		60		ns

∗ Pulsed: Pulse duration = 300 µs, duty cycle ≤ 1 %

TO-39 MECHANICAL DATA

DIM.	mm			inch		
	MIN.	TYP.	MAX.	MIN.	TYP.	MAX.
A	12.7			0.500		
B			0.49			0.019
D			6.6			0.260
E			8.5			0.334
F			9.4			0.370
G	5.08			0.200		
H			1.2			0.047
I			0.9			0.035
L	45^{o} (typ.)					

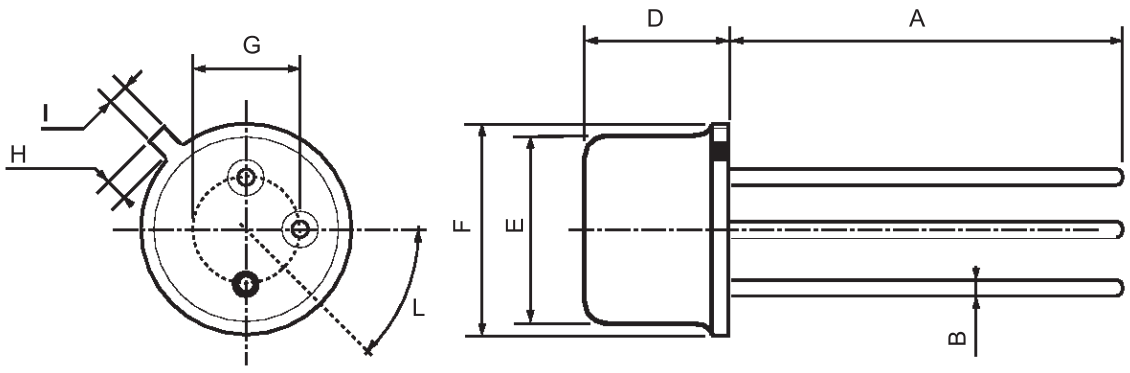

P008B

2N3055
MJ2955

COMPLEMENTARY SILICON POWER TRANSISTORS

- STMicroelectronics PREFERRED SALESTYPES
- COMPLEMENTARY NPN-PNP DEVICES

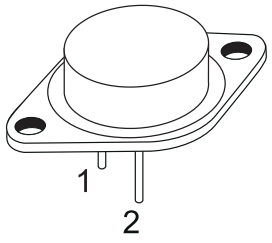

TO-3

DESCRIPTION

The 2N3055 is a silicon Epitaxial-Base Planar NPN transistor mounted in Jedec TO-3 metal case.

It is intended for power switching circuits, series and shunt regulators, output stages and high fidelity amplifiers.

The complementary PNP type is MJ2955.

INTERNAL SCHEMATIC DIAGRAM

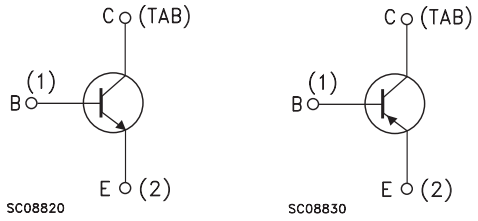

ABSOLUTE MAXIMUM RATINGS

Symbol	Parameter		Value	Unit
		NPN	2N3055	
		PNP	MJ2955	
V_{CBO}	Collector-Base Voltage (I_E = 0)		100	V
V_{CER}	Collector-Emitter Voltage ($R_{BE} \leq 100\Omega$)		70	V
V_{CEO}	Collector-Emitter Voltage (I_B = 0)		60	V
V_{EBO}	Emitter-Base Voltage (I_C = 0)		7	V
I_C	Collector Current		15	A
I_B	Base Current		7	A
P_{tot}	Total Dissipation at $T_c \leq 25\ ^oC$		115	W
T_{stg}	Storage Temperature		-65 to 200	^oC
T_j	Max. Operating Junction Temperature		200	^oC

For PNP types voltage and current values are negative.

THERMAL DATA

$R_{thj\text{-}case}$	Thermal Resistance Junction-case Max	1.5	°C/W

ELECTRICAL CHARACTERISTICS (T_{case} = 25 °C unless otherwise specified)

Symbol	Parameter	Test Conditions	Min.	Typ.	Max.	Unit
I_{CEX}	Collector Cut-off Current (V_{BE} = -1.5V)	V_{CE} = 100 V V_{CE} = 100 V T_j = 150 °C			1 5	mA mA
I_{CEO}	Collector Cut-off Current (I_B = 0)	V_{CE} = 30 V			0.7	mA
I_{EBO}	Emitter Cut-off Current (I_C = 0)	V_{EB} = 7 V			5	mA
$V_{CEO(sus)}$*	Collector-Emitter Sustaining Voltage (I_B = 0)	I_C = 200 mA	60			V
$V_{CER(sus)}$*	Collector-Emitter Sustaining Voltage (R_{BE} = 100 Ω)	I_C = 200 mA	70			V
$V_{CE(sat)}$*	Collector-Emitter Saturation Voltage	I_C = 4 A I_B = 400 mA I_C = 10 A I_B = 3.3 A			1 3	V V
V_{BE}*	Base-Emitter Voltage	I_C = 4 A V_{CE} = 4 A			1.8	V
h_{FE}*	DC Current Gain	I_C = 4 A V_{CE} = 4 A I_C = 10 A V_{CE} = 4 A	20 5		70	
f_T	Transition frequency	I_C = 0.5 A V_{CE} = 10 V	3			MHz
$I_{s/b}$*	Second Breakdown Collector Current	V_{CE} = 40 V	2.87			A

* Pulsed: Pulse duration = 300 µs, duty cycle 1.5 %
For PNP types voltage and current values are negative.

TO-3 MECHANICAL DATA

DIM.	mm			inch		
	MIN.	TYP.	MAX.	MIN.	TYP.	MAX.
A	11.00		13.10	0.433		0.516
B	0.97		1.15	0.038		0.045
C	1.50		1.65	0.059		0.065
D	8.32		8.92	0.327		0.351
E	19.00		20.00	0.748		0.787
G	10.70		11.10	0.421		0.437
N	16.50		17.20	0.649		0.677
P	25.00		26.00	0.984		1.023
R	4.00		4.09	0.157		0.161
U	38.50		39.30	1.515		1.547
V	30.00		30.30	1.187		1.193

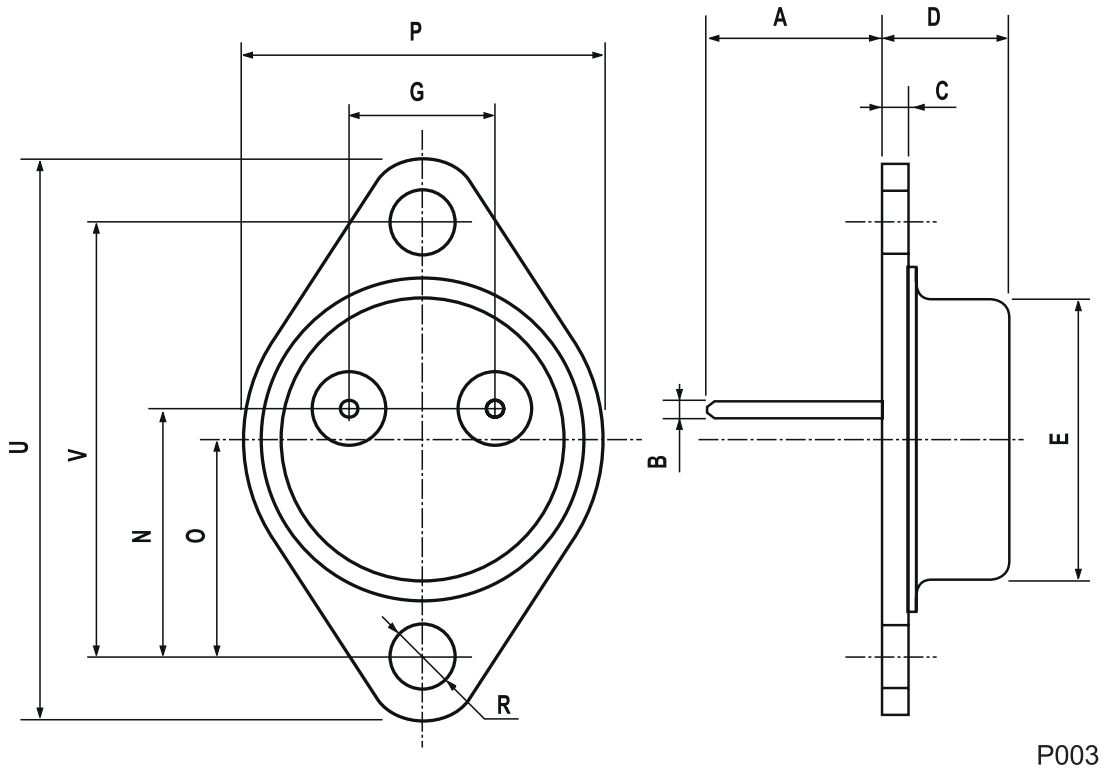

3.2.2 Connecting The Motor Driver

Caution

It is recommended that the MTS series stages be driven by the Thorlabs TDC001 DC Servo Motor Driver. If the stage is being driven by any other driver or controller, consult Section 6.1. for motor pin out details and Chapter 5 for details of the motor specification.

The stage is supplied with 0.5m (1.6 ft) of cable and is terminated in a 15 pin D-Type connector. This is compatible with the MOTOR drive terminal of the TDC001 T-Cube DC driver unit - see Fig. 3.1 below. A 3m (9.8 ft) extension cable (PAA632) is available on request

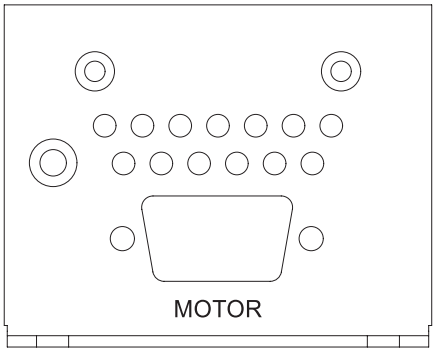

Fig. 3.1 TDC001 rear panel

3.2.3 Fitting and Removing the Base Plate

Referring to Fig. 3.2, proceed as follows:

1) Fit the dowels supplied to the base plate (MTS25A-Z8 or MTS50A-Z8).
2) Position the stage on the base plate, ensuring that the dowels locate correctly in the holes in the lower surface of the stage.
3) Fit the four bolts supplied M3 x 12 (4-40 x 1/2") through the holes in the underside of the base plate, and tighten to secure the stage in place.

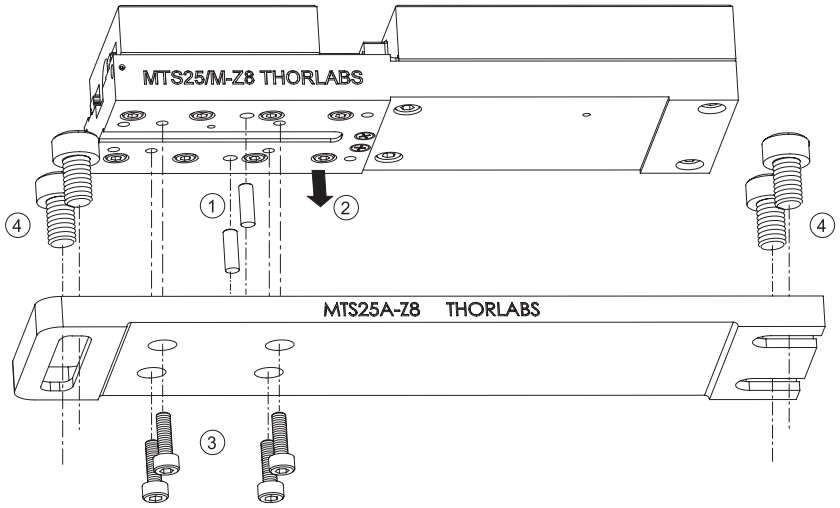

Fig. 3.2 Fitting the MTS25A-Z8 Base Plate

4) Fit two of the bolts supplied M6 x 10 (1/4-20 x 3/8") through each end of the base plate to fix the stage to the work surface.
5) To remove the base plate, reverse the procedure above.

3.2.4 Building an XY Configuration

Referring to Fig. 3.3, proceed as follows:

1) Fit the dowels supplied to the moving platform of the lower stage.
2) Note the orientation of the spacer plate in the drawing below, then fit the spacer plate (MTS25B-Z8 or MTS50B-Z8) to the moving platform of the lower stage, ensuring that the dowels locate correctly in the holes and protrude through the top surface of the spacer plate.
3) Fit the four bolts supplied M3 x 6 (4-40 x 1/4”), through the holes in the spacer plate, and tighten to secure the plate in place.
4) Fit the Y-axis stage into place ensuring that the dowels in the spacer plate locate correctly in the holes in the lower surface of the stage..

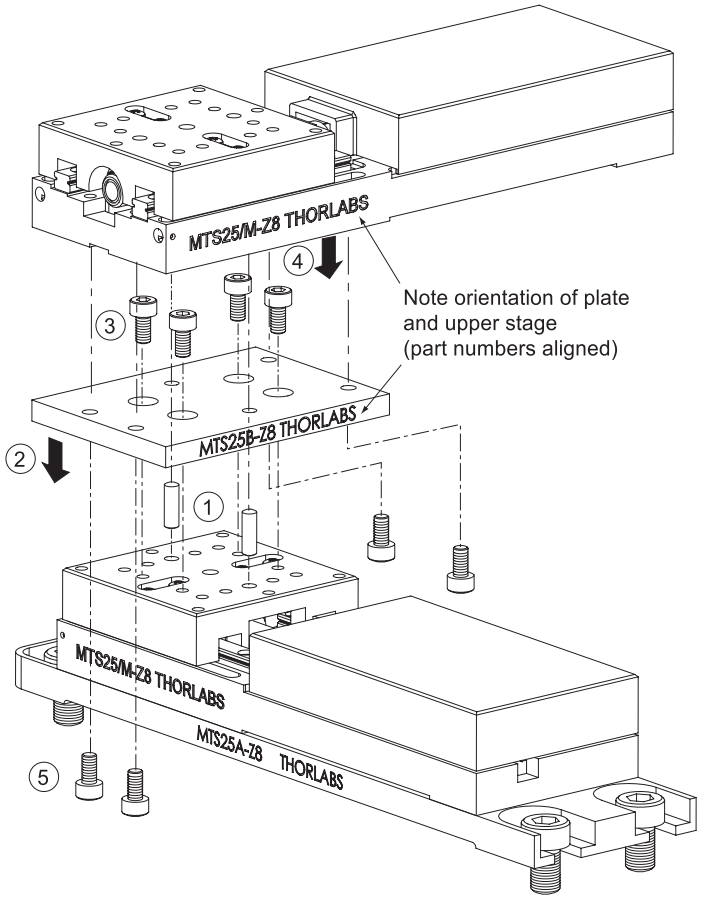

Fig. 3.3 Building an XY Configuration

5) Fit the four bolts supplied M3 x 6 (4-40 x 1/4”) through the holes in the underside of the spacer plate and screw into the base of the upper stage.
6) Tighten the bolts to secure the stage in place.
7) Fit the base plate to the X-axis (lower) stage, and bolt the assembly to the worksurface as detailed in Section 3.2.3.

3.2.5 Building an XYZ Configuration

Assemble an XY configuration as detailed in Section 3.2.4. then, referring to Fig. 3.4, proceed as follows:

1) Fit the shorter dowels supplied, into the moving platform on the upper stage of the XY assembly.
2) Fit the angle bracket (MTS25C-Z8 or MTS50C-Z8) onto the moving platform of the stage, ensuring that the dowels fitted at item (1) locate correctly in the holes on the underside of the angle bracket..

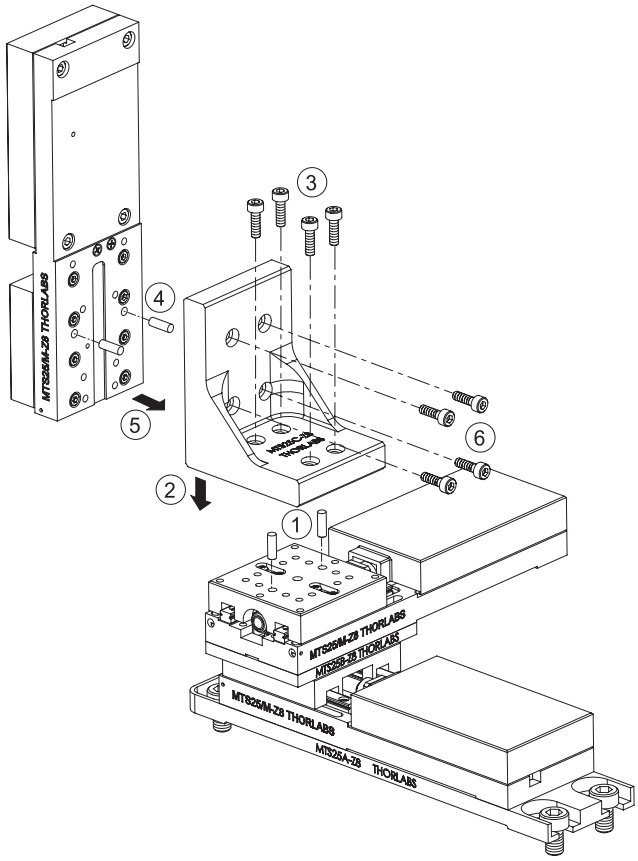

Fig. 3.4 Adding a Vertical Axis Stage

3) Fit the four bolts supplied M3 x 12 (4-40 x 1/2”), through the holes in the base of the angle bracket, and tighten to secure the bracket to the XY assembly.
4) Fit the longer dowels supplied to the underside of the base on the vertical-axis stage.
5) Fit the vertical-axis stage into place ensuring that the dowels fitted at item (4) locate correctly into the holes in the back surface of the angle bracket.
6) Fit the four bolts supplied M3 x 12 (4-40 x 1/2”), through the holes in the angle bracket, and screw into the base of the vertical-axis stage.
7) Tighten the bolts to secure the stage in place.
8) Fit the base plate to the X-axis (lower) stage, and bolt the assembly to the worksurface as detailed in Section 3.2.3.

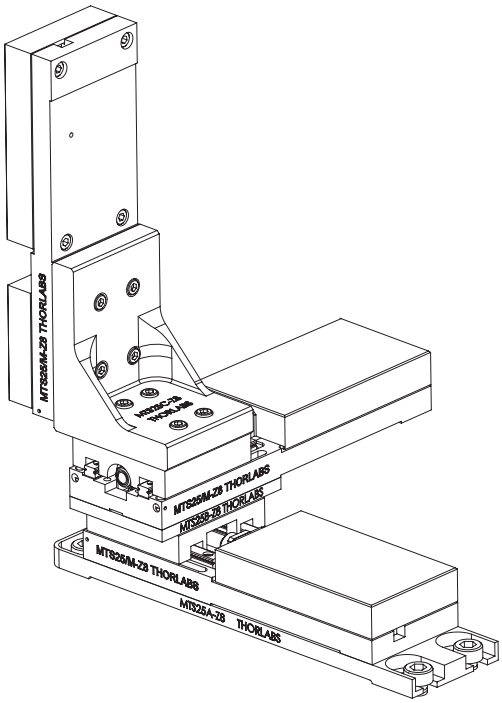

Fig. 3.5 Typical XYZ configuration

3.3 Transportation

Caution

When packing the unit for shipping, use the original packing. If this is not available, use a strong box and surround the unit with at least 100 mm of shock absorbent material.

3.4 Dimensions

3.4.1 MTS Dimensions

all dimensions in inches (mm)

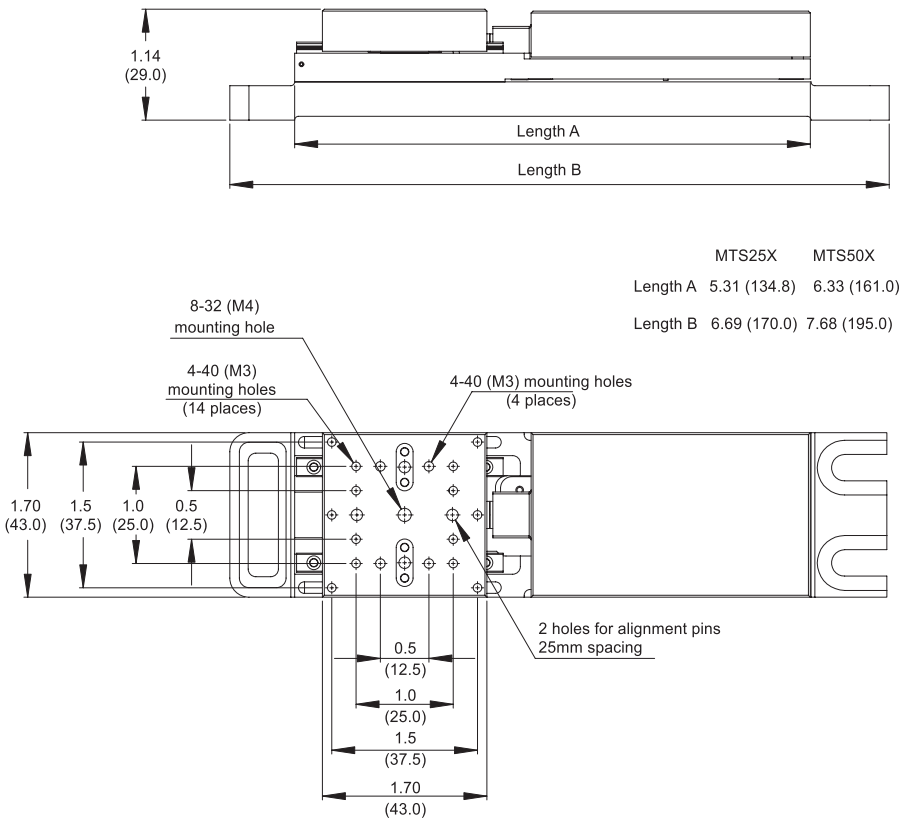

Fig. 3.6 Dimensions

Spectral Products

Spectrometers · Spectrophotometers · Color Instruments · Spectrographs · Monochromators

111 Highland Drive · Putnam, CT · 06260 · USA
PHONE (860) 928-5834· FAX (860) 928-2676
http://www.spectralproducts.com

SM242

Hand-held CCD Spectrometer

- *Compact system, pre-configured model, can be handheld*
- *Flexible optical input direct to slit or via fiber*
- *Designed from the ground up for a wide range of applications*
- *Impact resistance housing*
- *High performance electronics*
- *Standard design allows up to 200-1050nm range*
- *USB 2.0 interface with 16bit A/D resolution*

The Choice for Spectral Applications

The SM242 is a new compact, pre-configured design CCD Spectrometer for use with a PC. Based on SP's special optical bench design, it supports many different applications where spectral or color measurements are required, including high dynamic range applications

The SM242 can accept light directly through its built-in slit or via optical fiber. A removable faceplate allows the use of standard SMA 905, FC, and custom fiber connectors. This faceplate also allows direct attachment to dedicated systems and a number of SMX Accessories. The durable aluminum housing that encloses the SM242 provides stable optical bench operation over a wide range of temperatures.

Spectral Products

Spectrometers · Spectrophotometers · Color Instruments · Spectrographs · Monochromators

111 Highland Drive · Putnam, CT · 06260 · USA
PHONE (860) 928-5834· FAX (860) 928-2676
http://www.spectralproducts.com

General Description

The standard sensor array used is the Sony ILX 511. The array driver electronics have been designed for highly sensitive yet stable operation. This array (in conjunction with our special UV coating process and customized order sorting filters) allows up to a 850nm measurement window from 200nm to 1050nm (smaller measurement window sizes increase spectral resolution and light sensitivity). The design of the SM242 also allows use of custom arrays for special applications, including photodiode assemblies and alternative CCD arrays.

Standard interfaces to the SM242 include a USB 1.1/2.0 compatible interface with 16-bit extended dynamic range.

The SM242 is a pre-configured model, so if the desired wavelength range matches one of the standard wavelength ranges, SP can ship the unit within a couple of days.

Software support includes a SDK and DLLs for dedicated applications development and our SM32Pro Windows-based spectral acquisition and analysis software.

Software

- ✓ SM32Pro - Windows® 98, 2000, XP based software for data acquisition and analysis
- ✓ Transmission, reflectance, and absorbance measurements
- ✓ Data export, zoom in and out, spectrum overlays, and many more features
- ✓ Color analysis tools included
- ✓ Signal average and integration time control
- ✓ DLL libraries available for easy user software development in DOS and Windows®
- ✓ VC++/VB/Labview examples available

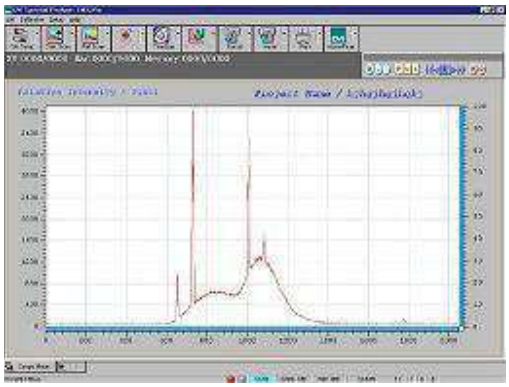

Software

Spectral Products

Spectrometers · Spectrophotometers · Color Instruments · Spectrographs · Monochromators

111 Highland Drive · Putnam, CT · 06260 · USA
PHONE (860) 928-5834· FAX (860) 928-2676
http://www.spectralproducts.com

Layout of SM242

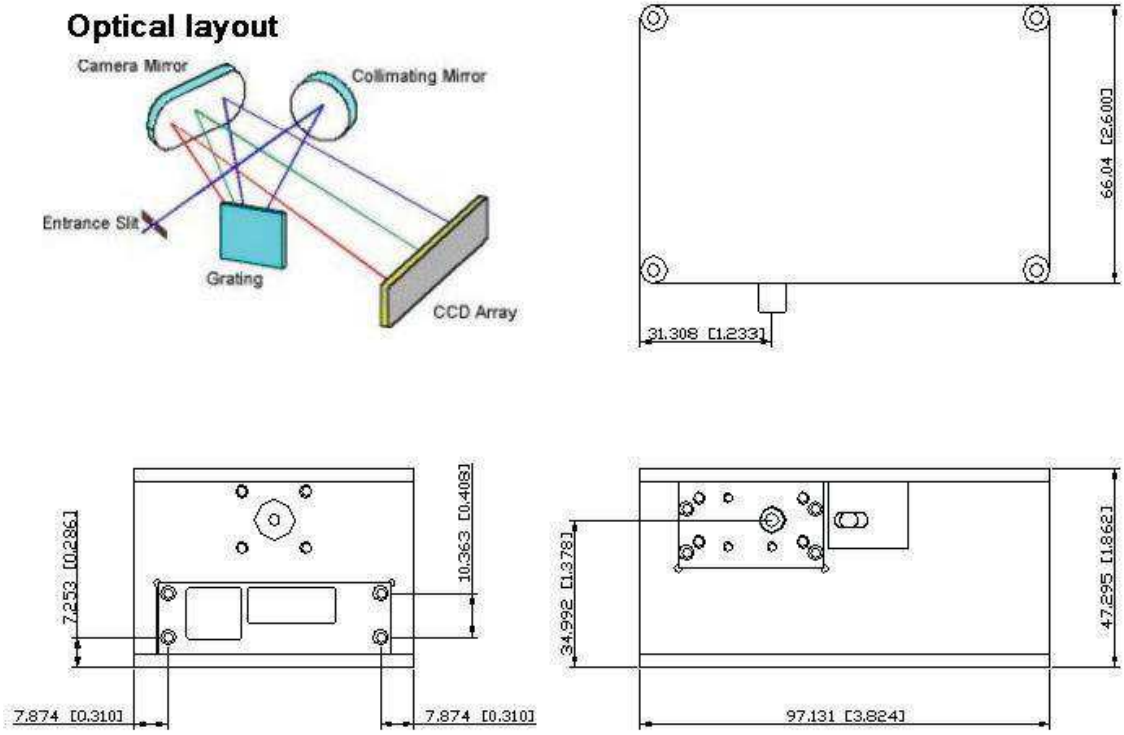

Specifications:

Detector: 2048 Sony CCD linear array
Pixel size: 14µm X 200µm
Sensitivity: 1800 V/(lx s) @ 660nm
Dimensions: 3.82”(H) X 2.60”(W) X 1.85”(D)
Weight: 0.5 lbs ARO.
Light Entrance:
- Slit: 10/25/50/100/200/400µm
- Fiber: SMA 905 or FC fiber coupler, 50-1000µm core fiber
- NA: 0.22

Stray light rejection: <0.1% (typical)
Spectral response range: 200 to 1050nm
Standard Spectral range:

200-400nm	200-450nm	200-600nm
350-700nm	380-760nm	400-800nm
650-1050nm	550-1050nm	350-1050nm
200-700nm	300-800nm	200-850nm
200-950nm	300-1050nm	200-1050nm

Spectral Resolution: ~0.1-10nm dependent on spectral range, slit width and fiber diameter
Grating: Ref, Appendix A
Interface: USB 2.0 480MHz/sec
A/D resolution: 16-bit
Integration Range: 1ms-65,536ms
Signal to Noise Ratio: >1000:1 (RMS), >300:1 (PV)
Temperature Range: 15-40°C

EXALOS
The bright light source company

NEW Driver Board Series EBD5010 (DIL), EBD5020 (BTF) EBD5080 (TOSA)

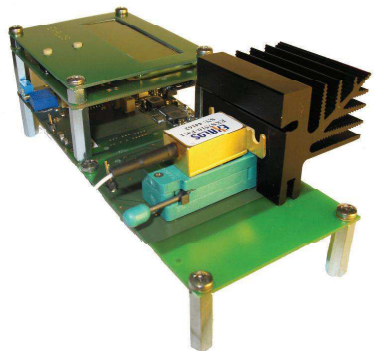

EXALOS new EBD5010, EBD5020 and EBD5080 Driver Boards are highly stable, ultra low noise solutions for R&D applications, allowing customers to easily change the light source, adjusting key parameters and control them via the on-board display.

APPLICATIONS

→ R&D Driver Board for semiconductor light sources

FEATURES

→ Driver Boards for DIL (EBD5010), BTF (EBD5020) and TOSA (EBD5080) modules
→ Generation of a highly stable, ultra-low noise drive current
→ Automatic current control (ACC) with stabilized feedback loop
→ High-performance temperature controller (5W, +/-0.001°C)
→ Current adjustment through external control voltage or on-board potentiometer
→ Light source enabling through mechanical code switch or TTL signal
→ Digital on-off modulation with TTL signal
→ Optional on-off modulation up to 10 kHz

TYPICAL PERFORMANCE

Part number	EBD5010/EBD5020/EBD5080
Driver Compliance	0–600 mA 1.0-2.7 V
Current Noise (1kHz-10MHz)	<150 µA rms
Current Stability Peak-to-Peak	0.07% in 1 hour 0.10% in 24 hours
Current Drift with Temperature	<10 µA/°C
Control Interface	analog in digital in/out
Temperature Range	-20 °C to +65 °C

EXALOS AG
Wagistrasse 21
CH-8952 Schlieren
Switzerland
Phone +41 43 444 60 90
Fax +41 43 444 6099
sales@exalos.com

EXALOS Inc.
60 Teal Drive
Langhorne, PA 19047
Phone +1 215 752 2115
Fax +1 215 752 3663
salesusa@exalos.com

www.exalos.com

3 EBD5000 DRIVER BOARD

3.1 PRINTED CIRCUIT BOARD (PCB)

The EBD5000 board has a size of 70 mm (L) x 55 mm (W). Fig. 1 shows pictures of the front side of the EBD5000 board. Fig. 2 shows a schematic top view of the board and the names of connectors, switches, potentiometers and LED indicators.

Fig. 1 Top view of the EBD5000 board

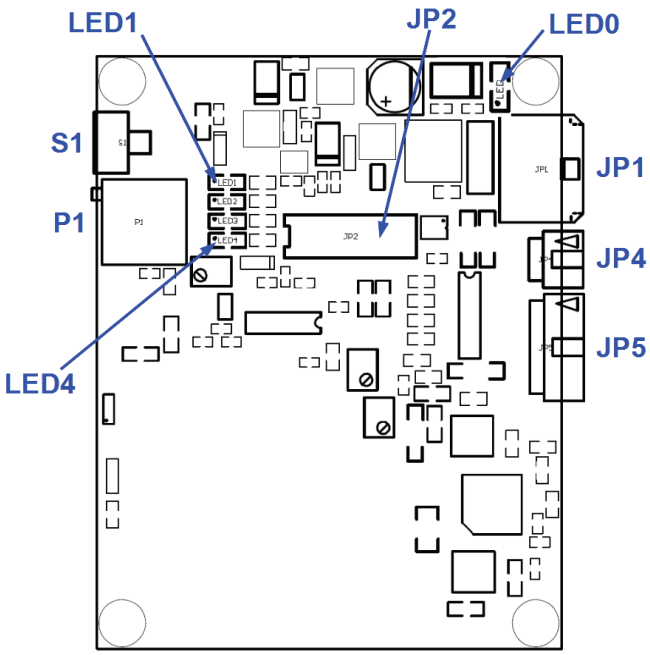

Fig. 2 Schematic top view of the EBD5000 indicating the user interfaces

3.2 ELECTRICAL USER INTERFACES

Different to the EBD5200, EBD5800 or similar OEM boards, the EBD5000 is not intended to be packaged in a metal case. Therefore, in principle, more connectors or status signals are available, for example the LED indicators or the JP2 connector to which a display board (DIB) can be connected. Table 1 provides a list of all electrical connectors that belong to the user interface.

Name	Connector on EBD5000 board	Function	Mating connector for cable assembly
JP1	MOLEX "Micro-Fit 3.0"; 43650-0300 Header (male)	+5V power supply, GND, PE	MOLEX "Micro-Fit 3.0"; 43645-0300 Receptacle (female)
JP2	Tyco "Micro-MaTch"; 1-215079-0 female-on-board	On-board diagnostics (for EXALOS use only)	Tyco "Micro-MaTch"; 8-215083-0 male-on-wire
JP4	MOLEX "Milli-Grid"; 87833-0420 Header (male)	SLED enable & on-off modulation	MOLEX "Milli-Grid"; 51110-0460 Crimp Housing
JP5	MOLEX "Milli-Grid"; 87833-1020 Header (male)	Analog and digital input & output signals	MOLEX "Milli-Grid"; 51110-1060 Crimp Housing

Table 1 List of electrical connectors (user interface)

Fig. 3 shows the front view of the connector JP1, JP4 and JP5. The corresponding pinout information is listed in Table 2, Table 3 and Table 4, respectively.

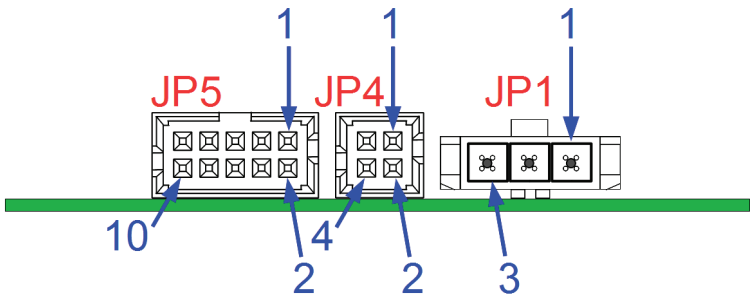

Fig. 3 Front view of header JP5, JP4 and JP1 with pin indication. The green bar indicates the PCB of the EBD5000.

Pin	Name	Description /Comment
1	PE	Protective Earth, to ground the metal case
2	GND	External electrical Ground
3	+5Vext	External 5V power supply (4.90-5.20 V)

Table 2 Pinout of header JP1

Pin	Name	Description / Comment
1	Modulation	5V TTL digital modulation signal
2	+5Vin	5V supply voltage from JP1, for configuration purposes only, e.g., enable the SLED through short to pin3
3	SLEDenable	5V TTL digital signal to enable/disable the SLED
4	GNDext	GND reference for Modulation or SLEDenable when realized with open-collector outputs, preferably not be used otherwise to avoid GND loops (use instead pin2 of JP1 as GND reference for Modulation and SLEDenable if possible)

Table 3 Pinout of header JP4

Pin	Name	Description / Comment
1	SLED_enabled	Open-collector output indicating SLED is on
2	AIN_enabled	Open-collector output indicating that SLED current is controlled through pin9/pin10
3	AIN_alarm	Open-collector output indicating excessive analog input voltage at pin9/pin10 is applied and limited to +2.5V
4	Temperature_alarm	Open-collector output indicating the read temperature of the SLED being either 1.5°C above or below the set temperature
5	GNDext	GND reference for pin1 to pin4
6	GNDext	GND reference for pin1 to pin4
7	AINenable	Enable SLED current control through pin9/pin10
8	+5Vin	5V supply voltage from JP1, for configuration purposes only, e.g., enable analog control through short to pin7
9	+AINextern	Analog input voltage (0-2.5V) to control SLED current
10	-AINextern	GND reference of analog input signal (pin 9)

Table 4 Pinout of header JP5

The right half of connector JP5 contains digital alarm or status signals that are decoupled from the rest of the electronics through opto-couplers. They are open-collector outputs with a common ground "GNDext" that is on pin5 and pin6 of JP5. These alarm signals are also logically connected to the four LEDs that are found on the board. As shown in Table 5, the pinout sequence of JP5 matches the configuration sequence of the LED indicators (except for power indicator LED0).

LED	Name	Description / Comment
LED0 (green)	Power	Indicating supply voltage with correct polarity after the fuse and brown-out and spike detector
LED1 (green)	SLED_enabled	Open-collector output indicating SLED is on
LED2 (orange)	AIN_enabled	Open-collector output indicating that SLED current is controlled through pin9/pin10
LED3 (orange)	AIN_alarm	Open-collector output indicating excessive analog input voltage at pin9/pin10 is applied and limited to +2.5V
LED4 (red)	Temperature_alarm	Open-collector output indicating the read temperature of the SLED being either 1.5°C above or below the set temperature

Table 5 Configuration of LED indicators

The left half of connector JP5 contains pins for analog control of the SLED drive current and hence of the optical output power. The analog input pins shall be handled with care as they are not decoupled through opto-couplers, which may, in cases of false connectivity, result in unwanted GND loops. Pin9 and pin10 allow for applying an analog control voltage (0 to +2.5V) in order to control the SLED current and to use the EBD5000 as part of an analog control loop. The analog control input voltage at +AINext and –AINext are fed into an instrumentation amplifier of high accuracy, low offset voltage and low drift.

Position	AINenable	SLEDenable	TECenable
0	Off	Off	On
1	Off	On	On
2	On	Off	On
3	On	On	On
4	Off	Off	Off
5	Off	On	Off
6	On	Off	Off
7	On	On	Off

Table 6 Configuration table for code switch S1

Table 6 shows possible configurations of the EBD5000 that can be selected through the code switch S1. The default configuration of S1 is '0', i.e. the temperature controller (TEC) is enabled but the SLED and the current control through an analog input signal is disabled. This means that the TEC is working as soon as a supply voltage is applied. The SLED is turned off and can be turned on through an active-HIGH (5V) signal on pin3 of JP4 or by switching the code switch S1 to '1'. The SLED current can be adjusted through the potentiometer P1.

Still, even in configuration '1' the SLED current can be adjusted electronically through pin9 and pin10 of JP5. In order to enable the control through an external analog signal an active-HIGH (5V) signal needs to be applied to pin7 of JP5, for example by shortening pin7 and pin8. In this case the setting of potentiometer P1 is ignored.

The TEC shall only be disabled for SLED modules not featuring a Peltier element. For standard BTF or DIL modules with an internal Peltier element the default configuration of S1 has the TEC enabled as it cannot be enabled electronically.

3.3 OPERATING CONDITIONS

Table 7 shows the typical, minimum and maximum operating conditions of the EBD5000 driver board.

Parameter	Min.	Typ.	Max.
Supply Voltage	4.9 V	5.0 V	5.2 V
Supply current, SLED disabled, TEC enabled (1)		0.3 A	2.0 A
Supple current, SLED enabled, TEC enabled (2)		0.8 A	3.0 A
Ambient operating temperature (3)	-20 °C		65 °C
Ambient storage temperature	-40 °C		85 °C

(1): Typical value at room temperature. Larger than typical supply currents can occur during power-up of the board or at extreme ambient temperatures.
(2): Typical value at room temperature and SLEDs up to 500 mA. Larger than typical supply currents can occur during power-up of the board or at extreme ambient temperatures.
(3): Extended temperature range from -40°C to +85°C available upon request.

Table 7 Operating conditions of the EBD5000

3.4 PERFORMANCE CHARACTERISTICS

Table 8 shows the typical performance of an EBD5000 driver board that was assessed with various short-wavelength and long-wavelength SLED modules from EXALOS. Furthermore, spectral noise measurements were performed with a high-precision electrical resistor and compared to optical relative intensity noise (RIN) measurements carried out with SLED modules.

During mid-term (up to 24 hours) experiments in an environmental chamber, measurements of the SLED current were performed every 6 seconds. The time-related drift was extracted through adjacent-averaging smoothing with a 1-hour window size (sliding-window averaging); the drift is not cumulative, i.e. drift over 24 hours can be zero. During mid-term and long-term (up to 1000 hours) experiments in a module test system, measurements of the SLED current and temperature were performed every 1 second and averaged over five minutes (300 samples) in order to record long-term trends.

Parameter (ptp=peak-to-peak, rms=root mean square)	**Typical**	**Maximum Rating**	**Conditions/Comments**
Drive current		600 mA	Extended current range up to 1000 mA upon request
Compliance voltage		3.0 V	
TEC current		1.8 A	Extended TEC currents up to 3.0 A upon request
TEC temperature stability ptp 24h	±0.002 °C	±0.01 °C	Equivalent to ±100 ppm @ 20 °C
TEC temperature drift 1000h	±0.07 ppm/h	±0.1 ppm/h	Linear interpolation over 1000 h
Current stability ptp 24h	±75 ppm	±100 ppm	Ambient temperature constant within ±0.5 °C
Current stability rms 24h	±20 ppm	±30 ppm	Ambient temperature constant within ±0.5 °C
Current stability ptp 1h	±75 ppm	±100 ppm	Ambient temperature constant within ±0.5 °C
Current stability rms 1h	±20 ppm	±30 ppm	Ambient temperature constant within ±0.5 °C
Mid-term current drift 24h	±9 ppm/h	±12 ppm/h	1h sliding window
Long-term current drift 1000h	±0.5 ppm/h	±0.8 ppm/h	Linear interpolation over 1000 h
Temperature-related current change (1)	±10 µA/°C	±15 µA/°C	Average value, not including warm-up
Current noise	1.3 μA_{rms}	1.5 μA_{rms}	Extracted from spectral noise measurements (1 kHz – 10 MHz)
Turn-on delay for SLED enable (2)	100 ms		
Turn-on delay on-off modulation (2)	10 ms		
10:90 rise time on-off modulation (2)	1 ms		
Max. on-off modulation frequency (3)	50 Hz		
Max. analog modulation frequency (3)	3 Hz		

(1): Typically a change of 1.0 mA or less in drive current is measured over temperature range from -40°C to +85°C.

(2): The EBD5000 features a built-in safety circuitry that powers down the electronic driver stage of the SLED whenever the SLED is disabled. This guarantees that under no circumstances the driver board can generate any light output from the SLED as long as the SLED is disabled. Furthermore, this turn-on delay also guarantees a controlled power-up behavior of the board in case the supply voltage is cycled while the SLED is enabled.

(3): The default configuration of the EBD5000 board is optimized for lowest possible noise performance with modulation rates of a few Hertz. The modulation switch on the board supports modulation rates up to 10 MHz and the default OpAmps support modulation rates up to 30 kHz. Upon request customized versions of the EBD5000 can be realized that support faster modulation rates, for example up to 10 kHz, at the expense of higher current noise.

Table 8 Typical performance characteristics of the EBD5000